Universiteit Leiden
The Netherlands

Herbivory-induced green leaf volatiles increase plant performance through jasmonate-dependent plant–soil feedbacks

Hu, L.; Zhang, K.; Xu, Y.; Zheng, X.; Waterman, J.M.; Ouyang, X.; ... ; Xu, J.

Citation
Hu, L., Zhang, K., Xu, Y., Zheng, X., Waterman, J. M., Ouyang, X., ... Xu, J. (2025). Herbivory-induced green leaf volatiles increase plant performance through jasmonate-dependent plant–soil feedbacks. *Nature Plants*, *11*(5), 1001-1017. doi:10.1038/s41477-025-01987-x

Version: Publisher's Version
License: Licensed under Article 25fa Copyright Act/Law (Amendment Taverne)
Downloaded from: https://hdl.handle.net/1887/4308994

Note: To cite this publication please use the final published version (if applicable).

nature plants

Article

https://doi.org/10.1038/s41477-025-01987-x

Herbivory-induced green leaf volatiles increase plant performance through jasmonate-dependent plant–soil feedbacks

Received: 8 October 2024

Accepted: 17 March 2025

Published online: 1 May 2025

Check for updates

Lingfei Hu[1] ✉, Kaidi Zhang[1,2,8], Yachun Xu[1,8], Xiaoxuan Zheng[1], Jamie M. Waterman[3], Xiao Ouyang[1,2], Zhenwei Wu[1], Zhicheng Shen[4,5], Yan He[1], Bin Ma[1], Christelle A. M. Robert[3], Jos M. Raaijmakers[6,7], Meng Ye[2] ✉, Matthias Erb[3] ✉ & Jianming Xu[1] ✉

Plants influence each other chemically by releasing leaf volatiles and root exudates, but whether and how these two phenomena interact remains unknown. Here we demonstrate that volatiles that are released by herbivore-attacked leaves trigger plant–soil feedbacks, resulting in increased performance of different plant species. We show that this phenomenon is due to green leaf volatiles that induce jasmonate-dependent systemic defence signalling in receiver plants, which results in the accumulation of beneficial soil bacteria in the rhizosphere. These soil bacteria then increase plant growth and enhance plant defences. In maize, a cysteine-rich receptor-like protein kinase, ZmCRK25, is required for this effect. In four successive year-field experiments, we demonstrate that this phenomenon can suppress leaf herbivore abundance and enhance maize growth and yield. Thus, volatile-mediated plant–plant interactions trigger plant–soil feedbacks that shape plant performance across different plant species through broadly conserved defence signalling mechanisms and changes in soil microbiota. This phenomenon expands the repertoire of biologically relevant plant–plant interactions in space and time and holds promise for the sustainable intensification of agriculture.

Plant–plant interactions drive ecosystem dynamics by structuring plant communities and modifying habitat properties. Plant chemicals that are released as leaf volatiles and soluble root exudates play an important role in this context, as they can reprogram the metabolism and growth of neighbouring plants[1–4].

Volatiles that are released by the leaves of herbivore-infested plants can be perceived by neighbouring plants. Herbivory-induced plant volatiles (HIPVs) not only exert direct toxic effects on insect herbivores[5,6] but also activate jasmonate-dependent defence pathways in neighbouring plants[7–10], which renders them more resistant to herbivore attack[11,12], thus enhancing their performance and fitness[13–16]. To date, a growing list of HIPVs, including terpenes, indole and green leaf volatiles, have been identified as active HIPVs that can trigger defence responses[17–19]. However, most studies on volatile-mediated plant–plant interactions have focused on immediate responses of neighbouring plants[20]. Whether plant volatiles can also regulate the defences of succeeding plants over broader time frames and spatial dimensions remains unexplored[21]. Addressing this gap is crucial for sustainable agriculture, as it affects the defence and yield of succeeding crops after crop rotation or continuous monocropping.

Exudates that are released by plant roots can alter the performance of neighbouring plants directly as well as indirectly through changes in the soil environment[2,22,23]. Root exudates are important drivers of plant–soil feedbacks (PSFs), which have strong impacts on plant fitness

A full list of affiliations appears at the end of the paper. ✉e-mail: lingfeihu@zju.edu.cn; yemeng@caas.cn; matthias.erb@unibe.ch; jmxu@zju.edu.cn

and yield, and consequently determine plant succession, plant diversity and community structure[24]. Changes in soil microbial communities often play an important role in these feedbacks[22]. In agriculture, PSFs are exploited through crop rotation to mitigate soil-borne diseases and improve crop yield[25,26].

Over the past decade, the mechanisms by which plants interact through aboveground volatiles have been gradually uncovered, and PSFs have been studied in detail in ecological and agricultural settings[22,27,28]. However, whether these two processes interact is unknown. Can leaf volatiles trigger PSFs that modify plant performance[21,27]? If yes, this may result in entirely new interaction patterns, extending volatile-mediated plant–plant interactions over much larger temporal scales[3]. The dynamics of these interactions could have important consequences for plant population and community dynamics across space and time[21] and could represent a powerful approach for the programming of crop plant successions and the sustainable intensification of crop production systems.

Here we conducted extensive laboratory and field experiments to comprehensively test whether and how HIPVs trigger PSFs across different plant species. We used CRISPR–Cas9 gene editing to modify volatile biosynthesis pathways to identify the active volatiles. Jasmonate-deficient mutants and pharmacological complementation allowed us to test whether the effect proceeds through canonical defence signalling. Soil microbiota profiling, isolation, sterilization and reinoculation experiments were employed to assess the contribution of root-associated microorganisms to the phenomenon. Finally, we used transcriptional profiling and gene editing to identify a receptor-like protein kinase (RLK) that mediates the response of plants to the changes in soil microorganisms. These experiments allow us to demonstrate that leaf volatiles trigger PSFs and thereby enhance the performance and yield of subsequent plants. This discovery connects two major types of plant–plant interactions and expands the impact of plant volatiles on plant performance across space and time, with potentially important ramifications for ecology and agriculture.

Results

Herbivory-induced green leaf volatiles promote plant performance via PSFs

To test whether HIPVs can modulate plant growth and defence via PSFs, we exposed maize plants to volatiles from herbivory-induced or non-induced sender plants, then removed the plants and grew new maize plants in the same soils (Fig. 1a and Extended Data Fig. 1a). Maize plants growing in soils of HIPV-exposed plants accumulated more biomass than plants growing in soils of control-exposed plants (Fig. 1b,c and Extended Data Fig. 1b). Fall armyworm (*Spodoptera frugiperda*) larvae grew less on plants growing in soils of HIPV-exposed plants and caused less damage (Fig. 1d,e). HIPV exposure thus changes soil properties in a way that enhances both the growth and herbivore resistance of the succeeding plants.

Which HIPVs are responsible for these PSFs? In the maize HIPV blend (Fig. 1b and Extended Data Fig. 1b), green leaf volatiles and indole are known to enhance maize defences[17,18]. To test for a potential role of indole, we knocked out the indole synthase Zm*IGL* using CRISPR–Cas9 gene editing (Extended Data Fig. 1c,d) and tested for the biological activity of indole-deficient HIPV blends. Receiver plants exposed to HIPV blends from indole-deficient *igl* mutant plants still triggered PSF effects (Fig. 1f–i). Thus, indole is not required for this process. To test for the contribution of green leaf volatiles to the observed feedbacks, we used green-leaf-volatile-deficient Zm*LOX10* mutant plants (Extended Data Fig. 1e,f). Receiver plants exposed to HIPV blends from green-leaf-volatile-deficient *lox10* mutant plants no longer triggered PSF effects (Fig. 1j–m). *lox10* mutant plants release no green leaf volatiles but also show reduced emission of other HIPVs (Extended Data Fig. 1f)[29]. Therefore, to further test for the role of green leaf volatiles in triggering PSFs, we exposed receiver plants to physiological concentrations of the three major green leaf volatiles, (*Z*)-3-hexenal (HAL), (*Z*)-3-hexen-1-ol (HOL) and (*Z*)-3-hexenyl acetate (HAC), after herbivory (Fig. 1n and Extended Data Fig. 1g–k). All three green leaf volatiles enhanced the growth and herbivore resistance of succeeding maize plants (Fig. 1o–q). Green leaf volatiles are thus both necessary and sufficient to elicit PSFs in maize.

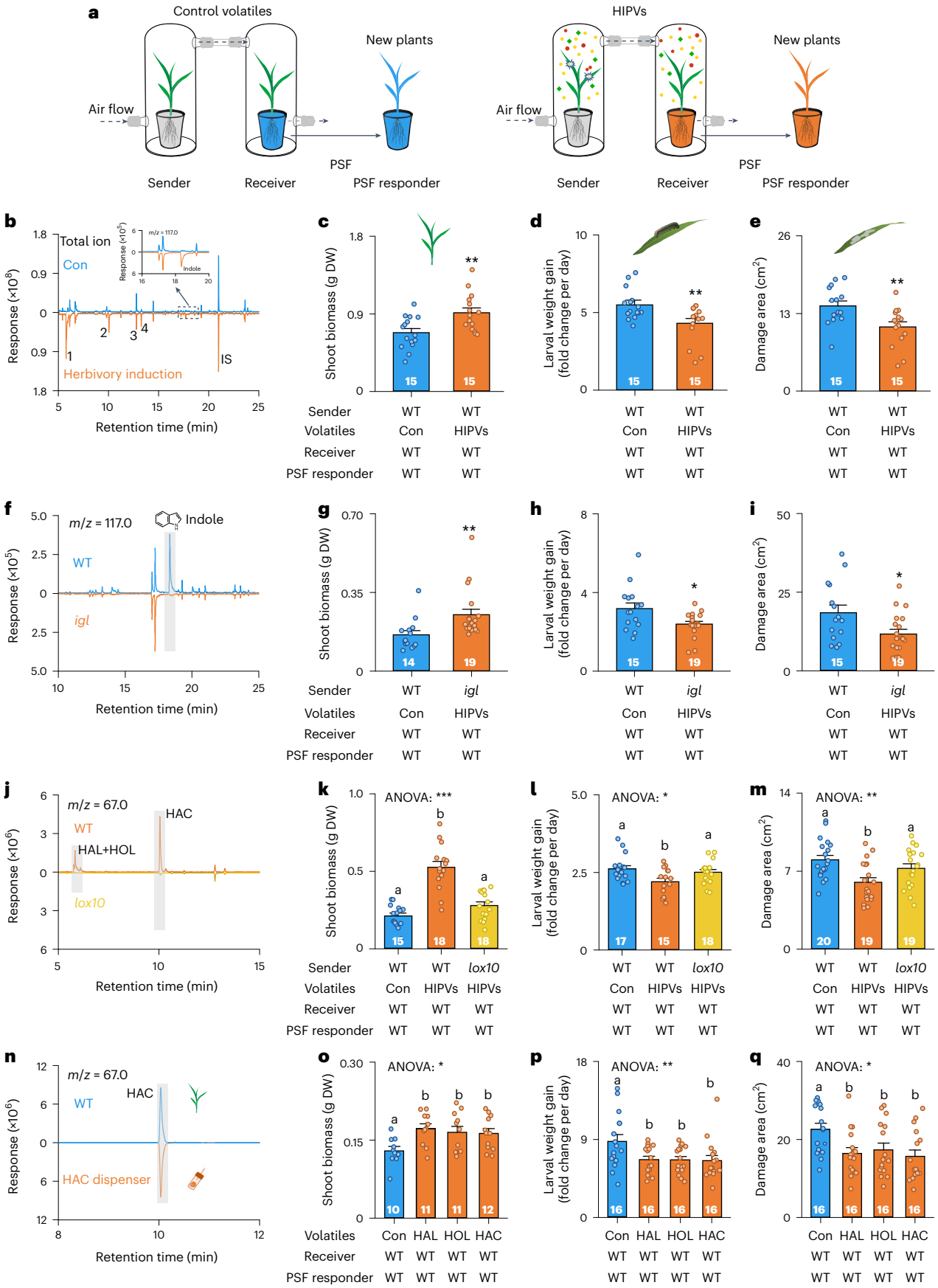
HAC-induced PSFs are conserved across plant species

After identifying the active volatiles, we conducted further experiments with synthetic HAC at physiological concentrations (Fig. 1n). As observed before, HAC-triggered PSFs resulted in increased shoot and root biomass, increased chlorophyll content, and decreased *S. frugiperda* growth and damage (Fig. 2a and Extended Data Fig. 2a–c).

To evaluate the robustness of the observed growth and resistance phenotypes, we performed a fully independent repetition of the above experiment in a different laboratory using a different soil and different growth conditions. As *S. frugiperda* was unavailable at this site, we used larvae of the beet armyworm (*Spodoptera exigua*). The experiment captured the resistance phenotype observed before: HAC exposure triggered PSFs, which decreased *S. exigua* growth and damage (Extended Data Fig. 2d–f). We also observed a tendency for maize plants to accumulate more biomass, but the effect was more variable and not statistically significant (Extended Data Fig. 2d–f). To account for this environmental variation, we included the full complement of growth and resistance phenotypes in subsequent experiments.

Fig. 1 | Herbivory-induced green leaf volatiles promote plant performance and resistance via PSFs. a, Set-up used for the volatile exposure experiment. Plants were placed in glass bottles with continuous airflow. Sender plants were either treated with simulated herbivory or left untreated. Receiver plants were exposed to the airflow from the sender plants for 1.5 h. After exposure, the receiver plants were removed, and new plants were planted in the same soils. **b**, Gas chromatography/mass spectrometry (GC/MS) total ion chromatograms of control (Con) and herbivory-induced WT sender plants. 1, HAL and HOL; 2, HAC; 3, linalool; 4, 4,8-dimethyl-1,3(*E*),7-nonatriene; IS, internal standard. **c**–**e**, Shoot biomass (**c**), caterpillar weight gain (**d**) and leaf damage (**e**) of WT plants growing in soils of Con- or HIPV-exposed receiver plants. The data are presented as mean + s.e.m. The exact number of biological replicates is indicated on each bar. The data points represent individual replicate samples. The asterisks denote significant differences between treatments (two-sided Student's *t* test; $^{**}P < 0.01$). DW, dry weight. **f**, GC/MS selected ion chromatograms of herbivory-induced WT and *igl* sender plants. **g**–**i**, Shoot biomass (**g**), caterpillar weight gain (**h**) and leaf damage (**i**) of WT plants growing in soils of receiver plants exposed to Con or HIPVs (from *igl* mutant plants). The data are presented as mean + s.e.m. The exact number of biological replicates is indicated on each bar. The data points represent individual replicate samples. The asterisks denote significant differences between treatments (two-sided Student's *t* test; $^{*}P < 0.05$; $^{**}P < 0.01$). **j**, GC/MS selected ion chromatograms of herbivory-induced WT and *lox10* sender plants. **k**–**m**, Shoot biomass (**k**), caterpillar weight gain (**l**) and leaf damage (**m**) of WT plants growing in soils of receiver plants exposed to Con or HIPVs (from *lox10* mutant plants). The data are presented as mean + s.e.m. The exact number of biological replicates is indicated on each bar. The data points represent individual replicate samples. Different letters denote significant differences between treatments (analysis of variance (ANOVA) followed by multiple comparisons of least squares means (LSMeans) corrected for false discovery rate (FDR); $P < 0.05$). Asterisks indicate overall ANOVA significance ($^{*}P < 0.05$; $^{**}P < 0.01$; $^{***}P < 0.001$). **n**, GC/MS selected ion chromatograms of herbivory-induced WT plants and capillary dispensers releasing synthetic HAC. **o**–**q**, Shoot biomass (**o**), caterpillar weight gain (**p**) and leaf damage (**q**) of WT plants growing in soils of Con- or HOL/HAL/HAC-exposed receiver plants. The data are presented as mean + s.e.m. The exact number of biological replicates is indicated on each bar. The data points represent individual replicate samples. Different letters denote significant differences between treatments (ANOVA followed by multiple comparisons of FDR-corrected LSMeans; $P < 0.05$). Asterisks indicate overall ANOVA significance ($^{*}P < 0.05$; $^{**}P < 0.01$). Raw data and exact *P* values for all comparisons in this figure are provided in Source Data Fig. 1.

https://doi.org/10.1038/s41477-025-01987-x



https://doi.org/10.1038/s41477-025-01987-x

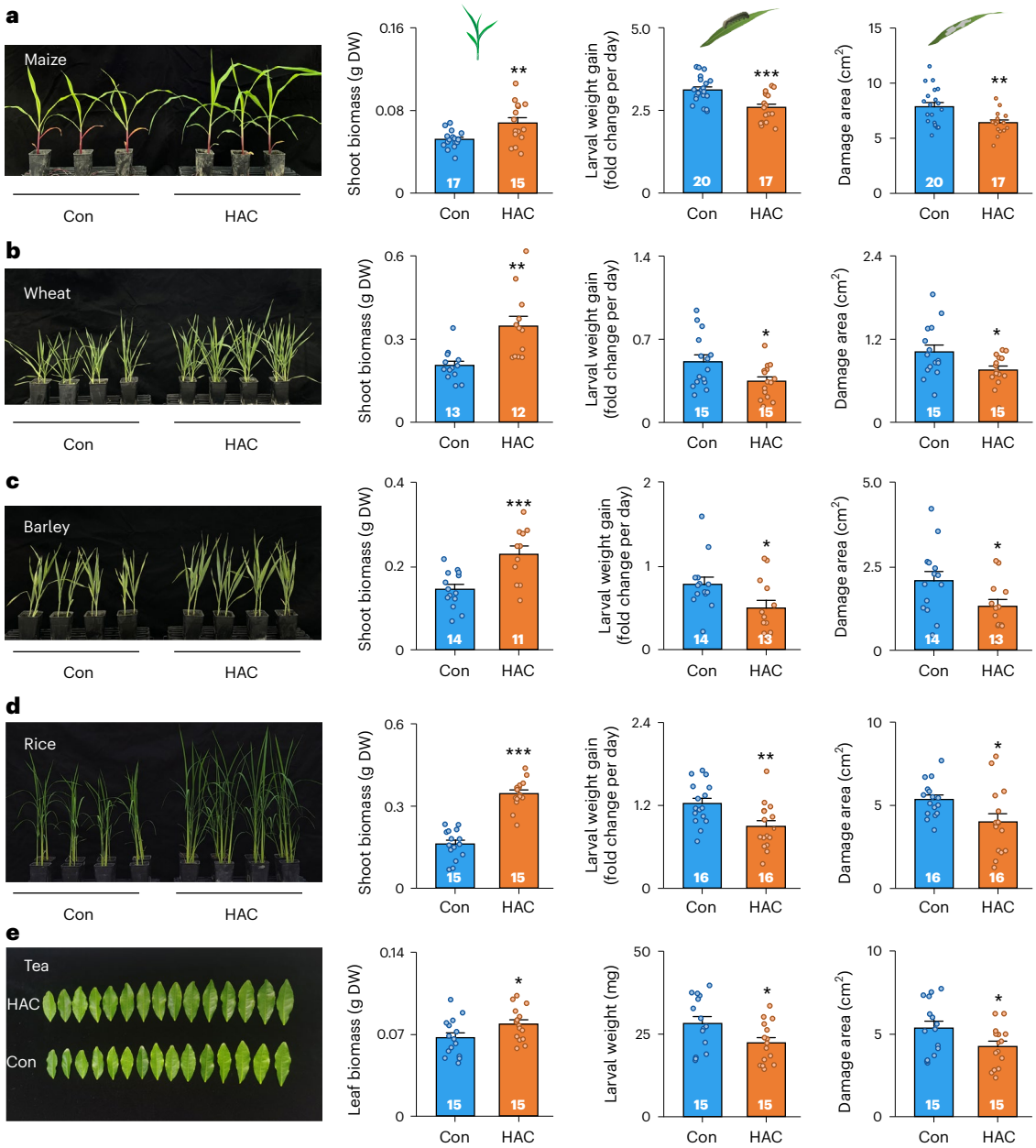


Fig. 2 | HAC-induced PSFs are conserved across different plant species. **a**–**e**, Growth phenotypes, shoot biomass, caterpillar weight gain and leaf damage of maize (**a**), wheat (**b**), barley (**c**), rice (**d**) and tea (**e**) plants growing in soils of Con- or HAC-exposed maize receiver plants. The data are presented as mean + s.e.m. The exact number of biological replicates is indicated on each bar. The data points represent individual replicate samples. The asterisks denote significant differences between treatments (two-sided Student's *t* test; $^{*}P < 0.05$; $^{**}P < 0.01$; $^{***}P < 0.001$). Raw data and exact *P* values for all comparisons in this figure are provided in Source Data Fig. 2.

HAC may trigger PSFs by directly interacting with the soil rather than the receiver plant. To test this possibility, we exposed soil to HAC without a receiver plant present and then measured soil feedback effects in the succeeding plants. We observed no changes in growth or resistance, showing that a receiver plant is necessary to trigger volatile-mediated PSFs (Extended Data Fig. 2g–i).

To further explore the parameter space in which HAC triggers PSFs on growth and defence, we varied the HAC exposure time of receiver plants, the soil incubation time of receiver plants after HAC exposure and the legacy time between the removal of the receiver plants and the addition of succeeding plants. We found that HAC exposure time and legacy time had no major influence on the feedback effects (Extended Data Fig. 3a–f). However, the incubation time of the receiver plants determined whether the feedback effects occurred or not. Leaving receiver plants for 6 h in the soil after 1.5 h of HAC exposure did not lead to significant feedback effects, while leaving the receiver plants for 24 h in the soil after 1.5 h of HAC exposure did result in significant effects (Extended Data Fig. 3h–i). Volatile-mediated PSFs thus require extended contact between the volatile receiver plant and the soil.

To test whether the PSF effect triggered by HAC is specific to maize, we performed feedback experiments with wheat, barley, rice and tea plants. HAC exposure of maize receiver plants enhanced growth and resistance in all five tested plant species grown in these conditioned soils (Fig. 2b–e).

To test feedback effects between plant species, we exposed rice plants to rice HIPVs and measured maize performance in rice-conditioned soils. Maize plants exhibited enhanced growth and resistance when grown in soils conditioned by HIPV-exposed rice plants

https://doi.org/10.1038/s41477-025-01987-x

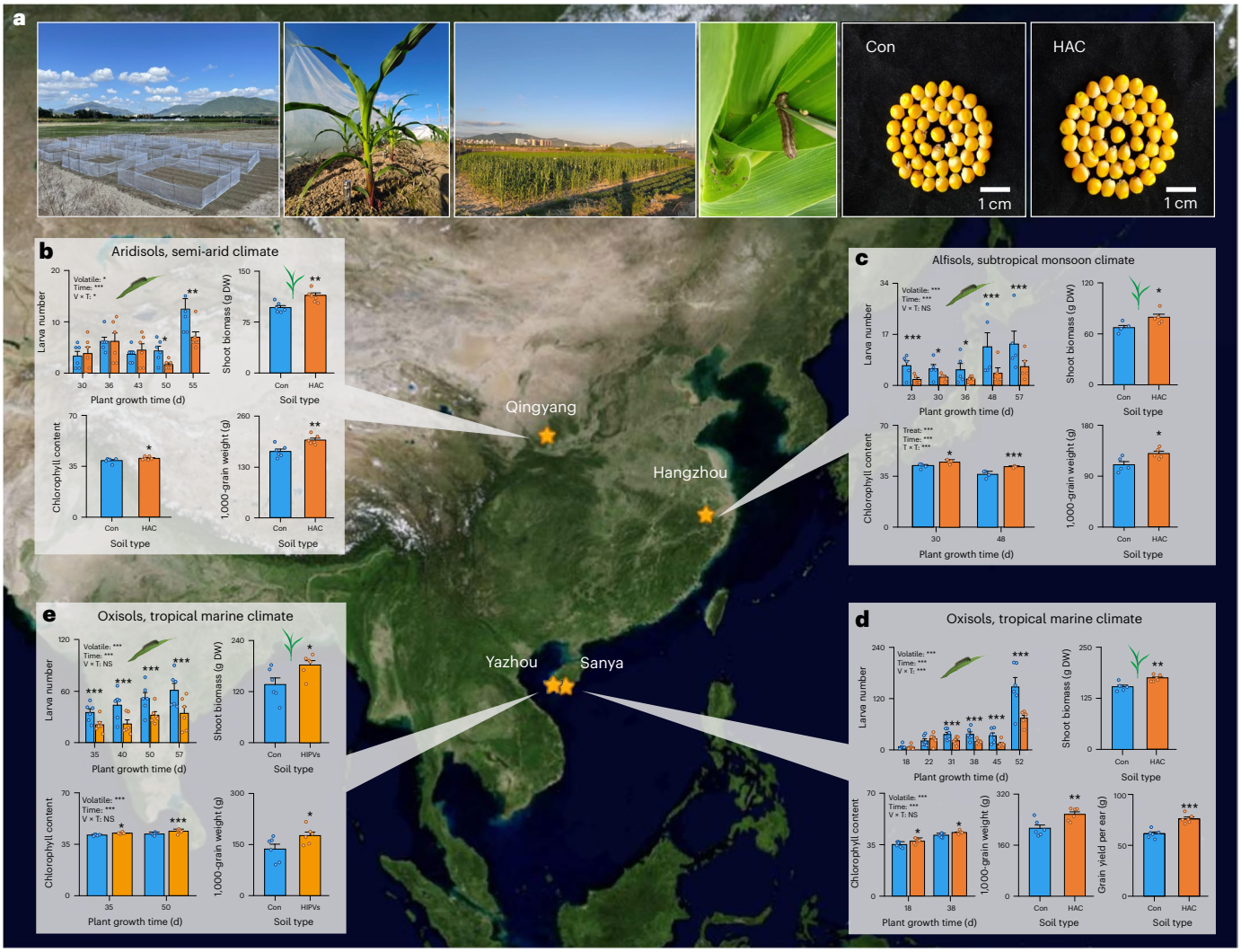


Fig. 3 | Herbivory-induced green leaf volatiles increase maize performance and yield in the field via PSFs. a, First panel: experimental set-up for HAC exposure in the field. Second panel: a maize plant exposed to an HAC dispenser. Third panel: new maize plants growing in the field. Fourth panel: a fall armyworm larva feeding on a maize plant. Fifth and sixth panels: seeds from maize plants growing in soils of Con- or HAC-exposed receiver plants. **b**–**d**, Number of fall armyworm larvae, shoot biomass, chlorophyll content and 1,000-grain weight of maize plants growing in soils of Con- or HAC-exposed receiver plants in Qingyang (**b**), Hangzhou (**c**) and Sanya (**d**). Total grain yield per ear was quantified in the field experiment in Sanya. The data are presented as mean + s.e.m. The field experiments in Qingyang included six biological replicates, while those in Hangzhou included five biological replicates. Each biological replicate represents one plot with 420 plants. The data points correspond to individual replicate samples. The asterisks indicate significant differences between treatments. Differences in larval number (**b**–**d**) and chlorophyll content (**c**,**d**) were analysed via ANOVA followed by pairwise comparisons of FDR-corrected LSMeans (*$P < 0.05$; **$P < 0.01$; ***$P < 0.001$). Differences in shoot biomass (**b**–**d**), chlorophyll content (**b**), 1,000-grain weight (**b**–**d**) and grain yield per ear were analysed using a two-sided Student's *t* test (*$P < 0.05$; **$P < 0.01$; ***$P < 0.001$). Note that Qingyang, Sanya and Hangzhou have distinct soil types and climates as indicated. The soil properties of these three locations are shown in Extended Data Fig. 5. NS, not significant. **e**, Number of fall armyworm larvae, shoot biomass, chlorophyll content and 1,000-grain weight of maize plants growing in soils of Con- or HIPV-exposed receiver plants in Yazhou. In this experiment, the receiver plants were naturally exposed to HIPVs from maize plants elicited by simulated herbivory. The data are presented as mean + s.e.m. and include six biological replicates. Each biological replicate represents one plot with 420 plants. Differences in larval number and chlorophyll content were analysed via ANOVA followed by pairwise comparisons of FDR-corrected LSMeans (***$P < 0.001$). Differences in shoot biomass and 1,000-grain weight were analysed using a two-sided Student's *t* test (*$P < 0.05$). Raw data and exact *P* values for all comparisons in this figure are provided in Source Data Fig. 3.

(Extended Data Fig. 4a–c). To further consolidate the cross-species effects, we exposed tea plants to tea HIPVs. We found that maize plants grown in the soils conditioned by HIPV-exposed tea plants also showed increased growth and resistance (Extended Data Fig. 4d,e). Taken together, these findings show that the response to volatile-induced changes in soil properties is conserved across different plant species.

Green leaf volatiles promote maize performance in the field via PSFs

We next investigated whether HIPV and HAC exposure can trigger significant PSFs in the field. We tested three different soil types and climatic conditions across China over four different years (Extended Data Fig. 5). In 2023, we elicited full HIPV blends in maize plants through simulated herbivory in Yazhou (oxisols, tropical marine climate; Fig. 3e). The full blend of HIPVs emitted by the sender plants primarily includes green leaf volatiles, aromatic compounds and terpenoids[30]. One day later, we removed the sender and receiver seedlings and planted new maize plants in the conditioned soil. Fall armyworm was the major insect herbivore in the field, and we thus analysed its abundance on new maize plants. Other herbivores such as beetles and stem borers were occasionally observed, but their abundance was too low for meaningful analysis. Maize plants growing in soils conditioned by HIPV receiver

https://doi.org/10.1038/s41477-025-01987-x

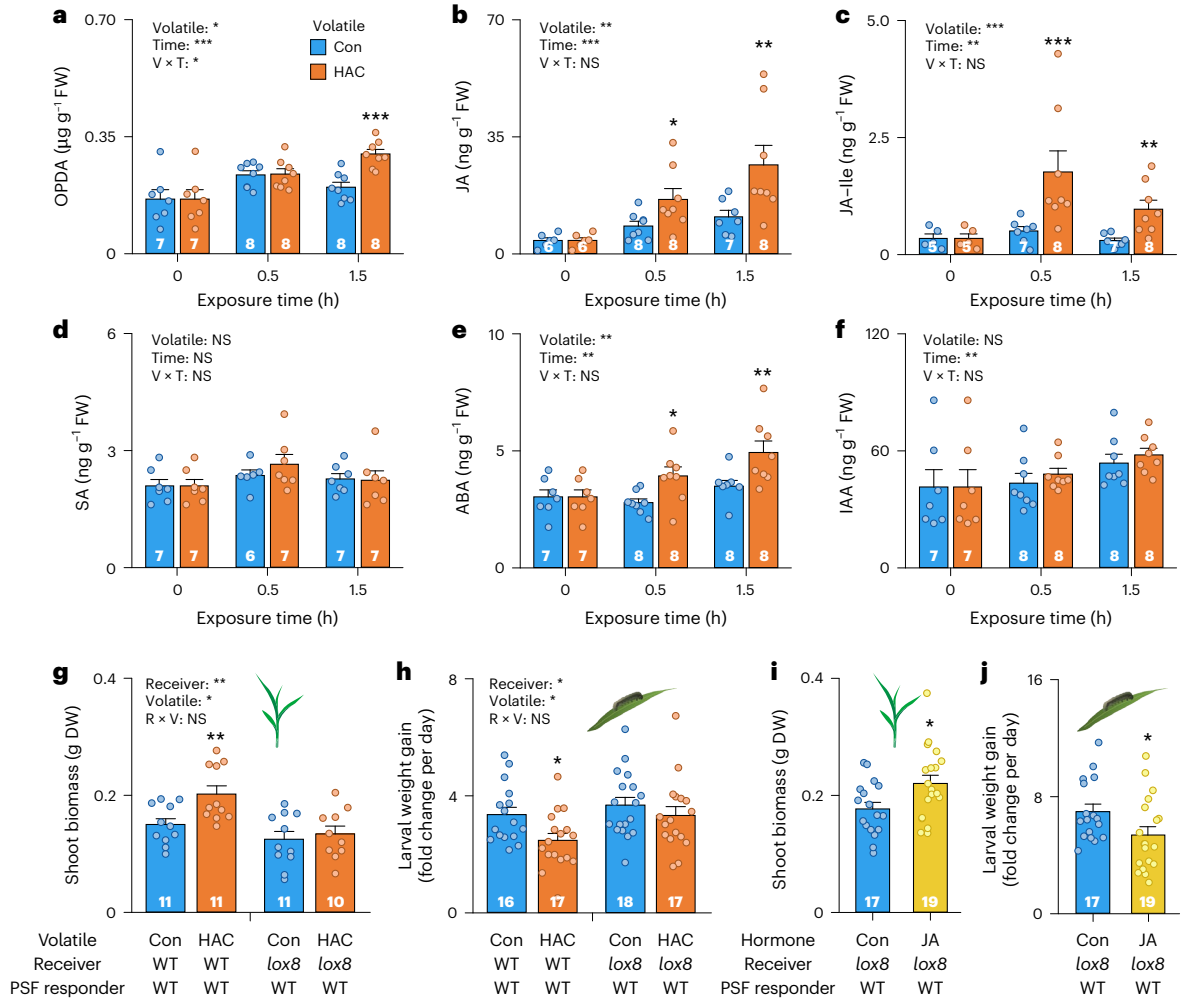


Fig. 4 | HAC triggers PSFs via systemic jasmonate signalling. a–f, Concentrations of OPDA (**a**), JA (**b**), JA–Ile (**c**), SA (**d**), ABA (**e**) and IAA (**f**) in the roots of Con- and HAC-exposed maize plants at different time points. The data are presented as mean + s.e.m. The exact number of biological replicates is indicated on each bar. The data points represent individual replicate samples. The asterisks denote significant differences between treatments (ANOVA followed by pairwise comparisons of FDR-corrected LSMeans; $*P < 0.05$; $**P < 0.01$; $***P < 0.001$). **g**,**h**, Shoot biomass (**g**) and caterpillar weight gain (**h**) of WT plants growing in soils of Con- or HAC-exposed WT or jasmonate-deficient *lox8* receiver plants. The data are presented as mean + s.e.m. The exact number of biological replicates is indicated on each bar. The data points represent individual replicate samples. The asterisks denote significant differences between treatments (ANOVA followed by pairwise comparisons of FDR-corrected LSMeans; $*P < 0.05$; $**P < 0.01$). **i**,**j**, Shoot biomass (**i**) and caterpillar weight gain (**j**) of WT maize plants growing in soils of Con- or JA-complemented *lox8* receiver plants. The data are presented as mean + s.e.m. The exact number of biological replicates is indicated on each bar. The data points represent individual replicate samples. The asterisks denote significant differences between treatments (two-sided Student's *t* test; $*P < 0.05$). Raw data and exact *P* values for all comparisons in this figure are provided in Source Data Fig. 4.

plants exhibited lower fall armyworm infestation, increased chlorophyll content, greater shoot biomass and higher grain weight (Fig. 3e). Thus, HIPVs can trigger PSFs that enhance maize resistance and yield.

To test whether HAC is sufficient to elicit these responses, we tested HAC triggered PSFs in three field experiments from 2020-2022, encompassing locations in Qingyang (aridisols, semi-arid climate), Hangzhou (alfisols, subtropical monsoon climate), and Sanya (oxisols, tropical marine climate). Maize seedlings were exposed to HAC dispensers for 1.5 h three times over three consecutive days. Following this exposure, the seedlings were removed, and new maize plants were planted. Maize plants growing in soils of HAC-exposed receiver plants had lower fall armyworm infestation, particularly in the later stages of the growing season (Fig. 3a–d). Shoot biomass and chlorophyll levels were consistently increased, together with grain weight. We also measured total grain yield per ear at one site and found a significant increase in plants growing in soils of HAC-exposed receiver plants (Fig. 3a–d). Thus, HAC exposure is sufficient to trigger positive PSF effects in the field.

HAC triggers PSFs via jasmonate signalling in receiver plants

HAC is known to induce jasmonate signalling in maize, which may trigger changes in root physiology[31]. We thus hypothesized that systemic HAC-induced jasmonate signalling may trigger PSFs. In line with this hypothesis, we found that HAC exposure significantly increased jasmonate levels in the roots of volatile receiver plants, including concentrations of 12-oxophytodienoic acid (OPDA), jasmonic acid (JA) and JA–isoleucine (JA–Ile) (Fig. 4a–c). Abscisic acid (ABA) levels were also increased, while salicylic acid (SA) and indole-3-acetic acid (IAA) levels remained unaffected (Fig. 4d–f). Since some phytohormones can be exuded from roots into the rhizosphere[32], we further explored whether HAC exposure triggers phytohormone release. We found that JA and JA–Ile levels were significantly increased in the rhizosphere soil of receiver plants after HAC exposure (Extended Data Fig. 6a). These results suggest a potential involvement of jasmonate signalling.

To test the hypothesis that jasmonates mediate volatile-induced PSFs, we used jasmonate-deficient *lox8* mutant plants as receiver plants. Jasmonate levels were significantly reduced in the roots of *lox8*

mutants, and the induction of OPDA, JA and JA–Ile by HAC was minor compared with wild-type (WT) plants (Extended Data Fig. 6b–e). *lox8* mutant plants failed to convey HAC into soil feedback effects on plant growth and resistance (Fig. 4g,h). Adding lanolin paste with synthetic JA to the stems of *lox8* mutants restored the growth and resistance phenotype of the succeeding plants (Fig. 4i,j).

To further substantiate the central role of jasmonate signalling in triggering PSFs, we exposed WT rice plants and the jasmonate-deficient *aoc* mutant to HIPVs[33] and assessed the performance of maize plants growing in the conditioned soils. Maize plants that grew in soils conditioned by HIPV-exposed WT rice plants displayed enhanced growth and resistance. Both effects disappeared when they grew in soils that were conditioned by *aoc* rice mutants (Extended Data Fig. 4a–c). Overall, maize plants growing in the soils of *aoc* mutants had lower growth and less resistance to herbivores (Extended Data Fig. 4a–c). Jasmonate signalling is thus both sufficient and required for HIPV- and HAC-mediated PSFs across different plant species.

Soil bacteria mediate HAC-triggered PSFs

Soil microorganisms, including bacteria and fungi, are responsive to hormonal changes in roots[34] and can mediate PSFs[35,36]. We thus hypothesized that HAC may trigger PSFs by changing soil microbiota. To test this hypothesis, we sterilized soils following exposure to control- and HAC-induced receiver plants and measured whether sterilization affects the feedback effects. We also complemented the sterilized soils with microorganism suspensions of non-sterilized soils of control and HAC-treated plants[22]. Feedback effects on growth and resistance disappeared in sterilized soils and reappeared in soils complemented with microorganism suspensions (Fig. 5a,b). These experiments show that an intact soil microbiota is required for volatile-mediated PSFs.

To test whether HAC treatment alters the composition of root-associated microbiota, we profiled fungal and bacterial communities in the rhizospheres of control- and HAC-exposed maize plants. Alpha diversity of both bacteria and fungi was not affected by HAC treatment (Fig. 5c and Extended Data Fig. 6f). Unconstrained principal coordinate analysis (PCoA) of Bray–Curtis distances revealed two distinct treatment clusters for both bacteria and fungi (Fig. 5d and Extended Data Fig. 6g). The differences in the root microbiota between control and HAC treatments were significant and detectable at the phylum, genus and operational taxonomic unit (OTU) levels (Fig. 5e–g, Extended Data Fig. 6h–j and Supplementary Data 1). Co-occurrence networks based on relative genus abundances revealed marked treatment differences in topological features for bacteria, with HAC treatment resulting in a more centralized network with more modularity (Fig. 5h and Extended Data Fig. 6i). Fungal co-occurrence networks showed no clear differences between treatments (Extended Data Fig. 6k–i). HAC treatment thus results in significant changes in the composition and network structure of root-associated microbiota.

To test the connections between changes in bacterial community composition and HAC-triggered PSFs, we cultured bacteria from the rhizospheres of control- and HAC-exposed plants. Cultivated bacteria that shared >98% 16S rRNA gene similarity with detected OTUs were used for further experiments. From the resulting collection of 102 strains, we selected 18 strains that corresponded to OTUs that were enriched in the rhizosphere of HAC-exposed plants (Supplementary Data 2). We then augmented soils with individual bacterial strains and quantified changes in growth and resistance. Five of the strains increased shoot biomass accumulation, and seven strains reduced leaf damage and growth of fall armyworm caterpillars (Fig. 5i and Extended Data Fig. 7a–l). Three strains, *Bacillus pacificus* strain2, *Priestia aryabhattai* and *Rossellomorea marisflavi*, increased both growth and resistance, similar to the PSFs induced by HAC. We used these three strains together with a fourth strain, *Priestia koreensis*, which did not modulate growth, in an additional complementation experiment. Soils were conditioned by control- or HAC-exposed plants, and we then complemented a subset of control soils with one of the four bacterial strains and measured the feedback effects. *Bacillus pacificus* strain2, *Priestia aryabhattai* and *Rossellomorea marisflavi* inoculations were sufficient to enhance maize growth and resistance similar to HAC treatment (Extended Data Fig. 7m,n). Together, the soil sterilization, microbiota profiling and bacterial inoculation experiments show that changes in the abundance of soil bacteria can explain HAC-induced PSFs.

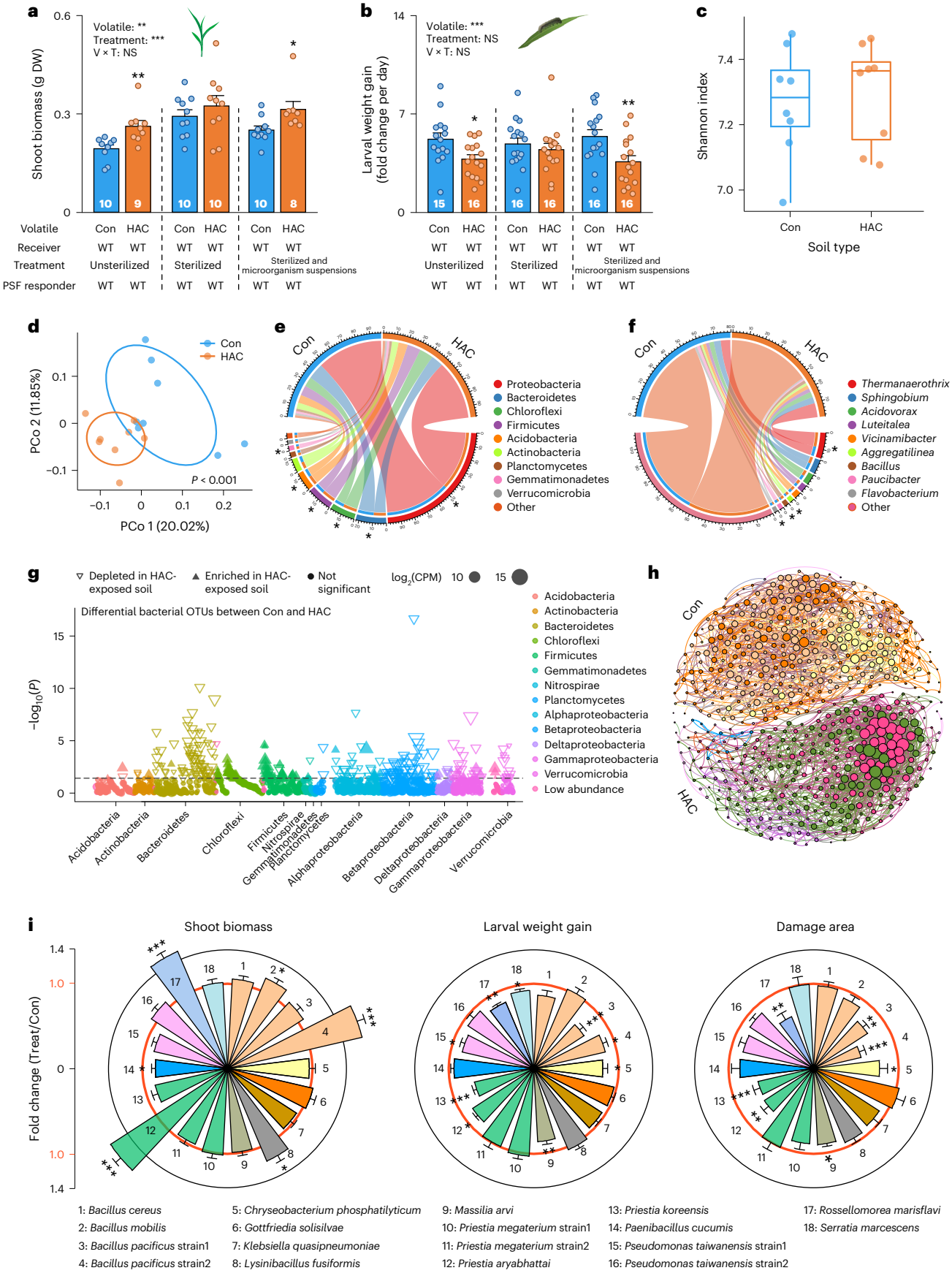
Jasmonate signalling mediates PSFs via soil bacteria

To clarify the connection between jasmonate signalling, soil microbiota and PSFs, we grew *lox8* plants in unsterilized and sterilized soils and complemented them with synthetic JA. JA-triggered feedbacks were present in non-sterilized soil but absent in sterilized soil (Extended Data Fig. 8a,b), indicating that the efficacy of jasmonate signalling in triggering PSFs is contingent on the presence of intact soil microbiota.

To investigate the impact of jasmonate signalling on soil microbiota, we profiled bacterial communities in the rhizospheres of both WT and *lox8* plants following HAC exposure. HAC treatment did not alter bacterial alpha diversity for either WT or *lox8* plants (Extended

Fig. 5 | Soil bacteria can mediate HAC-triggered PSFs. a,**b**, Shoot biomass (**a**) and caterpillar weight gain (**b**) of WT plants growing in soils of Con- or HAC-exposed receiver plants. Soils were left untreated, X-ray sterilized or X-ray sterilized and complemented with microorganism suspensions from the respective non-sterilized soils. The data are presented as mean + s.e.m. The exact number of biological replicates is indicated on each bar. The data points represent individual replicate samples. The asterisks denote significant differences between treatments (ANOVA followed by pairwise comparisons of FDR-corrected LSMeans; $^{*}P < 0.05$; $^{**}P < 0.01$; $^{***}P < 0.001$). **c**, Shannon index of bacterial communities in the rhizospheres of Con- and HAC-exposed maize receiver plants. There were eight biological replicates for each treatment. The data points represent individual replicate samples. The horizontal bars within the boxes represent the medians. The tops and bottoms of the boxes represent the 75th and 25th percentiles, respectively. The upper and lower whiskers extend to data no more than 1.5× the interquartile range from the upper and lower edges of the box. **d**, Unconstrained PCoA with Bray–Curtis distance showing that the rhizosphere bacterial communities of Con-exposed maize receiver plants separate from those of HAC-exposed receiver plants in the first axis ($P < 0.001$; permutational multivariate ANOVA by Adonis). There were eight biological replicates for each treatment. The data points represent individual replicate samples. **e**,**f**, Phylum-level (**e**) and genus-level (**f**) distributions of bacteria communities in the rhizospheres of Con- and HAC-exposed receiver plants. There were eight biological replicates for each treatment. Asterisks denote significant differences between treatments ($^{*}P < 0.05$, two-sided Wilcoxon rank-sum tests). **g**, Manhattan plot showing bacterial OTUs enriched in the rhizospheres of Con- or HAC-exposed receiver plants. Each dot or triangle represents a single OTU. Filled and empty triangles indicate OTUs enriched in Con- and HAC-exposed soils, respectively. Differential OTU abundance was analysed using two-sided Wilcoxon rank-sum tests, with *P* values corrected using the FDR method ($P < 0.05$). OTUs are arranged in taxonomic order and coloured according to the phylum or, for Proteobacteria, the class. The horizontal dashed line indicates the threshold *P* value ($P = 0.05$) for statistical significance. CPM, counts per million. **h**, Rhizobacterial co-occurrence networks of Con- and HAC-exposed receiver plants. The networks were constructed on the basis of Spearman correlation analysis of taxonomic profiles ($P < 0.05$). The nodes in the network represent genera, and links indicate potential microbial interactions. Node size is proportional to degree. **i**, Fold changes of the shoot biomass, larval weight gain and damage area of WT plants inoculated with different bacterial strains, which correspond to the OTUs that are enriched in the rhizosphere of HAC-exposed plants. The data are presented as mean + s.e.m. For the full datasets, including the exact number of biological replicates, refer to Extended Data Fig. 7. Fold-change values above 1.0 indicate increased plant growth, larval weight gain and leaf damage, while values below 1.0 indicate reduced levels of these parameters. The asterisks denote significant differences between treatments (two-sided Student's *t* test; $^{*}P < 0.05$; $^{**}P < 0.01$; $^{***}P < 0.001$). Raw data and exact *P* values for all comparisons in this figure are provided in Source Data Fig. 5.

https://doi.org/10.1038/s41477-025-01987-x



https://doi.org/10.1038/s41477-025-01987-x

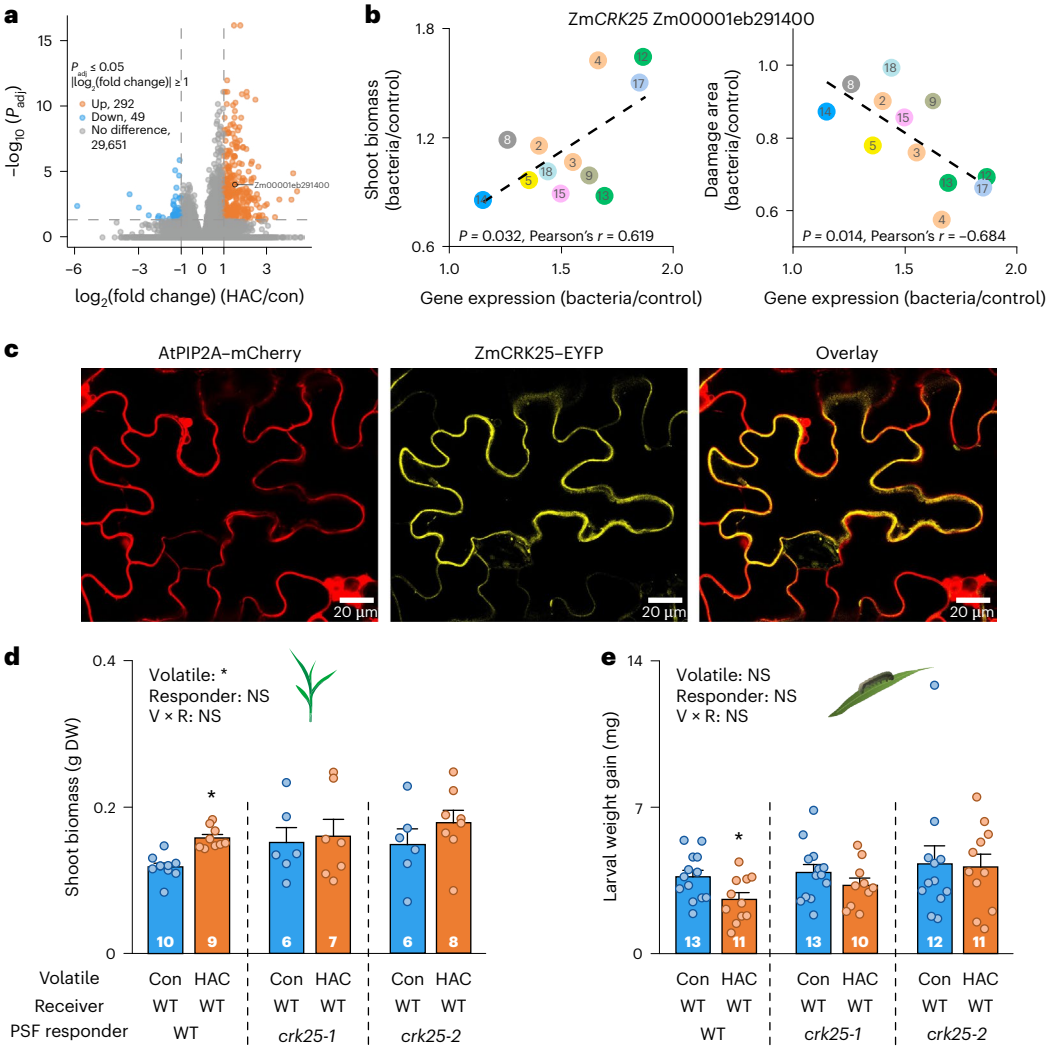


Fig. 6 | Soil bacteria mediate HAC-triggered PSFs via Zm*CRK25* in succeeding plants. a, Transcriptomic analyses of differentially expressed genes in maize roots grown in soils of Con- or HAC-exposed receiver plants. Con and HAC treatments included six and seven biological replicates, respectively. Orange features indicate genes more abundant in roots grown in soil of HAC-exposed receiver plants, while blue features indicate genes more abundant in roots grown in soil of Con-exposed receiver plants. Differential expression was analysed using DESeq2 (two-sided test), with *P* values adjusted using the FDR method ($P \le 0.05$ and $|\log_2(\text{fold change})| \ge 1.0$). **b**, Correlations between bacteria-triggered plant growth, damage area and Zm*CRK25* expression after inoculation with individual bacterial strains. The numbers on the points represent the bacteria strains that are enriched in the rhizosphere of HAC-exposed plants (Fig. 5i). The correlations were analysed using linear regression. Pearson's *r* and *P* values are shown. **c**, Subcellular localization of ZmCRK25. ZmCRK25–enhanced yellow fluorescent protein (EYFP) fusion was transiently expressed in the leaf epidermal cells of *Nicotiana benthamiana*. ZmCRK25–EYFP was colocalized with a known *Arabidopsis* plasma membrane marker, AtPIP2A–mCherry. From left to right are mCherry signal (red), YFP signal (yellow) and an overlay of the two signals. **d**,**e**, Shoot biomass (**d**) and caterpillar weight gain (**e**) of WT and Zm*CRK25*-knockout plants growing in soils of Con- or HAC-exposed receiver plants. The data are presented as mean + s.e.m. The exact number of biological replicates is indicated on each bar. The data points represent individual replicate samples. The asterisks denote significant differences between treatments (ANOVA followed by pairwise comparisons of FDR-corrected LSMeans; $^*P < 0.05$). Raw data and exact *P* values for all comparisons in this figure are provided in Source Data Fig. 6.

Data Fig. 8c). However, HAC exposure changed beta diversity in the rhizosphere of WT plants but not that of *lox8* mutants (Extended Data Fig. 8d). Furthermore, the more centralized co-occurrence network observed in WT plants after HAC exposure was entirely absent in the *lox8* mutants (Extended Data Fig. 8e). These findings show that HAC-induced jasmonate signalling is necessary to trigger significant changes in soil microbiota and microbiota-mediated PSFs.

Zm*CRK25* is required for HAC-triggered PSFs

How are soil microbial changes that are triggered by HAC translated into enhanced plant performance? To address this question, we conducted a comparative transcriptomic analysis of maize roots growing in soils conditioned by control- or HAC-exposed plants. Our analysis revealed 341 differentially expressed genes (Fig. 6a and Supplementary Data 3). Given the pivotal role of RLKs in perceiving extracellular stimuli, particularly in response to microbial interactions[37], we specifically focused on differentially expressed genes associated with plasma-membrane-localized RLKs. Within this subset, we identified 12 genes encoding RLKs, and 9 of them were predicted to be localized on the plasma membrane (Supplementary Data 3).

To assess the responsiveness of these nine RLKs to HAC-enriched bacteria, we quantified their expression levels in plant roots grown in soil that was individually inoculated with the 12 previously isolated bacterial strains using quantitative real-time PCR (Fig. 5i). The RLKs exhibited distinct responsiveness to the 12 bacterial strains (Extended Data Fig. 9a). Across different bacterial strains, the expression of Zm00001eb291400 showed a strong correlation with plant growth and herbivore resistance: strains that more effectively

https://doi.org/10.1038/s41477-025-01987-x

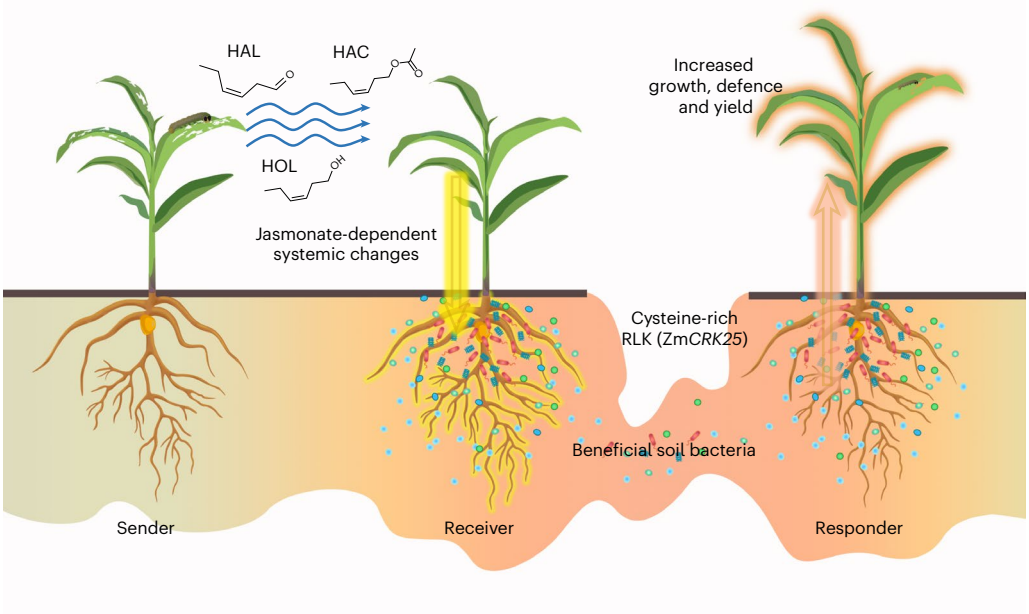


Fig. 7 | Proposed model for volatile-mediated PSFs. Upon herbivore attack, plants release green leaf volatiles including HAL, HOL and HAC. These green leaf volatiles induce jasmonates both locally and systemically in the roots of neighbouring plants. The resulting changes in root metabolism reprogram the composition of rhizosphere microorganisms, including the enrichment of growth- and defence-promoting bacteria. Their accumulation then increases the expression of a cysteine-rich RLK, Zm*CRK25*, and consequently enhances the performance of succeeding plants by reducing leaf herbivore damage and promoting plant growth. These PSFs operate in the field and can enhance maize yield.

promoted plant growth and defence induced stronger expression of Zm00001eb291400 after bacterial inoculation (Fig. 6b and Extended Data Fig. 9b). We thus hypothesized that Zm00001eb291400 might play a role in responding to HAC-enriched soil bacteria.

To test this hypothesis, we obtained the full-length complementary DNA of Zm00001eb291400 by reverse transcription PCR. The cDNA nucleotide sequence comprised an open reading frame of 2,067 bp, encoding a predicted protein of 688 amino acids with an estimated molecular mass of 74.1 kDa. Analysis of the deduced amino acid sequence predicted the presence of an amino-terminal extracellular region including a signal peptide, two salt stress response/antifungal domains (PF01657), a single transmembrane domain and a carboxy-terminal cytoplasmic serine/threonine kinases domain (Extended Data Fig. 10a). Its closest characterized homologues in *Arabidopsis thaliana* were identified as cysteine-rich RLKs (CRKs) containing At*CRK25*, At*CRK10* and At*CRK29* (Extended Data Fig. 10b). On the basis of these characteristics, we named Zm00001eb291400 'Zm*CRK25*'.

At*CRK10* and At*CRK29* have been reported to be strongly induced by bacterial pathogens such as flagellin, and activate plant defences against pathogens and herbivores[38–40]. To further explore the role of Zm*CRK25*, we investigated the subcellular localization of ZmCRK25. Using the membrane-localized marker AtPIP2A, we observed a fluorescent signal at the plasma membrane (Fig. 6c), suggesting that ZmCRK25 is localized in the plasma membrane.

To test the involvement of Zm*CRK25* in HAC-mediated PSFs, we generated Zm*CRK25*-knockout lines (*crk25-1* and *crk25-2*) using CRISPR–Cas9 gene editing and stable transformation (Extended Data Fig. 10c) and evaluated their response to HAC-induced soil conditioning. The feedback effects triggered by HAC on plant and herbivore growth disappeared in the Zm*CRK25*-knockout lines (Fig. 6d–e). Thus, Zm*CRK25* is required for the volatile-mediated PSFs on growth and defence.

Discussion

Plants interact chemically with each other via leaf volatiles and root exudates[22,28,41,42]. However, little is known about how leaf volatiles shape plant–plant interactions across longer temporal scales, and whether they do so by influencing rhizosphere signalling. This study demonstrates that leaf volatiles can increase the growth and resistance of succeeding plants by triggering PSFs, thus revealing a new layer of chemically mediated plant–plant interactions (Fig. 7).

Volatile-mediated PSFs are mediated by green leaf volatiles and jasmonates, which are both highly conserved across the plant kingdom and generally induced by wounding and herbivore attack[10,43,44]. Green leaf volatiles, as ubiquitous phytochemical cues, align with the concept of conserved signals driving ecological processes, as discussed by Frost[45]. These signals facilitate interactions with soil bacteria known to enhance plant performance[46–48], leading to increased growth and resistance in succeeding plants. Together with the fact that the observed PSFs are conserved across different experiments, soil types, environmental conditions and plants, including interactions between different plant species, this newly discovered phenomenon is likely to be widespread and may thus play an important role in determining (agro)ecosystem dynamics.

Different stress volatiles can influence plant growth and defence[7], and first (albeit contested) reports indicate that they may trigger systemic root signalling to influence root microbial composition[21,27]. Through the combined use of CRISPR–Cas9 gene editing of volatile biosynthesis and synthetic volatile complementation, we provide strong evidence that green leaf volatiles in HIPV blends trigger PSF effects. Green leaf volatiles trigger these feedbacks by systemically inducing the production and exudation of jasmonates in the roots and into the rhizosphere of receiver plants. Although our experiments demonstrate that green leaf volatiles and jasmonates are both necessary and sufficient, other volatiles (including terpenoids) and other plant hormones such as SA and ABA may play roles in different plant species and under different environmental conditions[19]. It would be worthwhile to explore the effects and mechanisms of other volatile signals in the future. Furthermore, whether jasmonates trigger feedbacks by changing other root exudate components remains to be determined.

Volatile exposure alters the composition of root-associated microbiota, including the enrichment of various rhizobacteria such as *Bacillus*, *Priestia* and *Pseudomonas* strains. Sterilization, complementation, isolation and enrichment experiments provide strong evidence for root microbiota changes as drivers of the observed feedback

effects. Individual rhizobacteria have been found to have such effects in earlier studies. For example, *Bacillus aryabhattai* LAD can promote maize growth and crop yield by synthesizing IAA and exopolysaccharides[47]. Furthermore, the rhizobacterium *Pseudomonas putida* KT2440 can prime systemic JA-dependent defence responses against maize anthracnose fungus[49]. While the role of individual rhizobacteria in interacting with plants is well understood, exploring the potential function of a synthetic community comprising a more diverse range of bacteria and fungi on maize seedlings represents an intriguing avenue for future research. Such experiments could also reveal whether the positive PSFs are the result of direct effects of the beneficial bacteria on the plant or the suppression of immunogenic/pathogenic strains via microbe–microbe interactions[50,51].

Plants rely on cell-surface-localized pattern recognition receptors to detect microbe-associated molecular patterns and consequently activate the immune response[37,52]. Here we discovered that HAC-triggered changes in soil microbiota induced the expression of an RLK called ZmCRK25. ZmCRK25 belongs to the cystine-rich RLK family due to its conserved cysteine motif (C-8X-C-2X-C) in the ectodomain. ZmCRK25 shows high similarity to At*CRK25*, At*CRK10* and At*CRK29* in *Arabidopsis*. At*CRK10* and At*CRK29* respond to bacterial pathogens such as flagellin and activate plant defence against pathogens and herbivores[38–40]. Similarly, ZmCRK25 localizes to the plasma membrane and exhibits a strong transcriptional response to soil bacteria. Furthermore, ZmCRK25 is required for translating HAC-mediated changes in soil microbiota into PSFs. ZmCRK25 may directly recognize signalling elements associated with microorganisms, such as microbe-associated molecular patterns, or indirectly be induced by other pattern recognition receptors and consequently elicit downstream responses. The identification of the ligands or interacting pattern recognition receptors of ZmCRK25 presents an exciting prospect for the future, which will contribute to a more comprehensive understanding of how soil microbiota supports the host immune system.

How might our work contribute to sustainable agricultural practices? We have demonstrated that volatile-mediated PSFs enhance maize performance and yield across different years and field sites. Such a pattern is highly desirable for crop production, as it may allow for reduced pesticide input and enhance yields[53]. Remarkably, farmers may have leveraged wound-induced PSFs through traditional practices. In the Song dynasty, approximately 1,000 years ago, the poet Dongpo Su wrote '君欲富饼饵, 要须纵牛羊', suggesting that introducing cattle and goats into wheat fields could lead to better wheat yields the following year. In Europe, rolling is sometimes conducted in winter wheat fields during certain stages to increase tillering[54]. Apart from additional fertilization and the breaking of apical dominance, both practices result in plant damage and the release of green leaf volatiles, thus potentially triggering PSFs. Our work thus provides an intriguing additional factor that may render these agricultural practices beneficial beyond current theory.

We propose two potential strategies to harness volatile-mediated PSFs for sustainable agriculture. First, one could deploy synthetic green leaf volatiles into the field, which may benefit both the current crop by enhancing biological control[15,55,56] and the next crop via PSFs. Second, it may be possible to trigger feedbacks directly in the crop by wounding it at the right growth stage. Rolling and grazing, for instance, as described above, could be optimized towards such effects. We acknowledge that our experimental set-up differs from traditional crop rotation practices; however, our findings provide important insights into how green leaf volatiles and JA-dependent signalling influence plant–soil interactions, which could have implications for both monocropping and rotational agricultural systems. Substantial additional work is required to put our results into practice. This includes the development of innovative volatile delivery systems such as slow-release formulations or bio-based carriers, which can be seamlessly integrated into existing farming practices without extensive manual intervention. Additionally, further research is needed to optimize the application of plant volatiles in agricultural settings, considering factors such as application timing, dosage and compatibility with existing crop management practices[15]. The cysteine-rich RLKs, such as Zm*CRK25* identified in our study, may represent attractive targets for the genetic enhancement of the observed effects. Taken together, our work represents a proof of concept that will facilitate the translation of this newly discovered biological phenomenon into sustainable agricultural practices.

Methods

Instructions for the reproduction of the core experiment

To assist other research groups in replicating the key phenotype of this study, we prepared a series of illustrative videos and detailed instructions that go beyond the typical scope of methods sections. These instructions describe the protocol for HAC exposure of maize plants and the subsequent determination of PSF effects on the new plants. The instructions are available via figshare (https://doi.org/10.6084/m9.figshare.28444481).

Plants and insects

To investigate the impacts of HIPVs on succeeding plants, maize (*Zea mays*), rice (*Oryza sativa*, cultivar Zhonghua11), wheat (*Triticum aestivum*, cultivar Jimai22), barley (*Hordeum vulgare*, cultivar Eunova) and tea (*Camellia sinensis*, cultivar Longjing 43) were used in this study. The maize genotypes included the *igl* mutant and its corresponding WT (KN5585), the *lox10* mutant and its corresponding WT (B73), the *lox8* mutant and its corresponding WT (W22) and the *crk25* mutant and its corresponding WT (B73-329). The JA-biosynthesis rice mutant *aoc* and its corresponding WT Xiushui11 were provided by R. Li at Zhejiang University; information on this mutant is available in Xu et al.[33]. In our experiments, seeds were pre-germinated to ensure uniformity and minimize variability in initial seed germination rates, which could otherwise influence the experimental outcomes. This approach allowed us to focus on the specific effects of volatile-mediated PSFs on plant growth and defence, independent of germination variability. While pre-germination is not typical for field-grown maize or other crops, it is a standard experimental procedure to control for germination differences in controlled studies.

The knockout mutant *igl* was generated according to a published protocol[57]. Briefly, two 20-bp target sequences in the coding regions of the Zm*IGL* gene were selected and inserted into a *pCPB*–Zm*Ubi*-derived CRISPR–Cas9 binary vector. The constructed vectors were transformed into the receptor line KN5585 via *Agrobacterium tumefaciens*-mediated transformation. We selected the T-DNA-free lines that carry homozygous deletions at the target sites resulting in a frame shift of Zm*IGL* for further experiments (Extended Data Fig. 1c). The effects of the *igl* mutation on indole biosynthesis were confirmed by quantifying volatile profiles using the protocol described in the section 'Volatile profiling'.

The knockout mutant *crk25* was generated using the same protocols described above but with guiding sequences that specifically target the coding regions of Zm*CRK25*. Two T-DNA-free lines that carry homozygous deletions at the target sites resulting in a frame shift of Zm*CRK25* were selected for further experiments (Extended Data Fig. 10c).

The *lox10* mutant was obtained from the Maize EMS-Induced Mutant Database (http://maizeems.qlnu.edu.cn/). The *lox10* mutant has a single G-to-A mutation in exon 4 that leads to a premature termination codon of the Zm*LOX10* gene (Extended Data Fig. 1e). The effects of the *lox10* mutation on the biosynthesis of green leaf volatiles were confirmed by quantifying the volatile profiles using the protocol described in the section 'Volatile profiling'.

The *lox8* mutant was acquired from the Maize Genetics Cooperation Stock Center at University of Illinois at Urbana-Champaign (http://maizecoop.cropsci.uiuc.edu) as a mixture of WT, heterozygous and homozygous seeds. Homozygous individuals were genotyped with gene-specific primers and further selfed for experiments (Extended

Data Fig. 6a). The effects of the *lox8* mutation on jasmonate biosynthesis were confirmed by quantifying the levels of OPDA, JA and JA–Ile using the protocol described in the section 'Phytohormone analysis'.

Fall armyworm (*S. frugiperda*) and beet armyworm (*S. exigua*) larvae were reared on an artificial diet as previously described[58]. Tea geometrid larvae (*Ectropis oblique*) were originally collected from the Plantation Centre of Tea Research Institute, Chinese Academy of Agricultural Sciences, and reared in an insectary as described in Ye et al.[59].

Soil conditioning by volatile exposure

To explore the influence of HIPVs on the succeeding plants, we used a natural bulk soil. The soil was collected from a field in Hangzhou, China (30.3076° N, 120.0749° E). The bulk soil source had not been used for growing any crops during the collection season. The collected bulk soil was passed through a 4.75-mm sieve, air-dried for 48 h and put into clean 400-ml pots. Uniform pre-germinated B73 seeds were individually sowed in the pots. The pots were randomly placed on a greenhouse table (28 °C ± 2 °C, 55% relative humidity, 14:10 h light/dark), rearranged and watered as required.

When the third leaf of a maize plant was fully open (around 10 days after planting), the maize plant was exposed to HIPVs or synthetic HAC, HOL and HAL using a continuous-airflow system. The synthetic HAC (70 ng h^{-1}), HOL (15 ng h^{-1}) and HAL (50 ng h^{-1}) were released from dispensers at a physiological dose corresponding to amounts emitted by herbivore-attacked maize plants (Extended Data Fig. 1g–k)[56]. The details of the volatile exposure system and the volatile dispensers were described in Hu et al.[18]. After 1.5 h of exposure, the receiver plants were moved out of the airflow system. On the second day after exposure, the exposed plants were removed, and the soil was harvested for growing the succeeding plants (see 'Feedback experiment' below). Here we carefully removed the exposed plants from the soil, including their root systems, to ensure consistency and precision in assessing the effects of volatile-mediated PSFs. While this approach differs from common agricultural practices, where roots are often left in the soil, it was necessary to isolate and evaluate the specific effects of plant volatiles on soil microbial communities and subsequent plant performance. We acknowledge that leaving root residues in the soil could introduce additional factors, such as decomposing organic matter, which might enhance or confound the observed effects.

To facilitate the volatile exposure procedures, we also used a passively ventilated system to expose maize plants with HAC dispensers, as described in Ye et al.[60,61]. Briefly, ventilated plastic cylinders (40 cm tall, 4 cm in diameter, open at the top) were made of transparent plastic sheets. The cylinders were placed on the pots, and the plants were placed in the greenhouse for experiments. HAC or control dispensers were added into the cylinders. After 1.5 h of exposure, the cylinders were carefully removed. The soils of control- and HAC-exposed receiver plants were subjected to the feedback experiments (see 'Feedback experiment').

Volatile profiling

To determine the volatile bouquets of WT, *igl* or *lox10* plants, we elicited the plants via simulated herbivory. Briefly, the maize plants were treated by wounding two leaves over an area (~0.5 cm^2) on both sides of the central vein with a razor blade, followed by the application of 8 µl of *S. frugiperda* oral secretions. This treatment results in plant responses comparable to those under real herbivore attack (Extended Data Fig. 1a)[62,63]. Following herbivory, volatiles were collected using a dynamic headspace sampling system and Super-Q traps. Detailed information on the volatile sampling system and volatile analysis has been published elsewhere[61].

Feedback experiment

New, uniform and pre-germinated B73 seeds were individually sown in soils in which volatile-exposed receiver maize plants were previously grown. The plants were cared for as described above. The chlorophyll content, shoot and root biomass, and herbivore resistance were determined for these new maize plants.

The chlorophyll content and shoot and root biomass of each plant were recorded 25 days after planting. The chlorophyll content of the youngest fully developed leaf was determined using a SPAD-502 meter (Minolta Camera). The biomass was harvested, oven-dried at 60 °C for 3 days and then weighed.

To explore the PSF effect triggered by HAC on other plant species, we performed experiments with wheat, barley, rice and tea plants. The shoot biomass and herbivore resistance of wheat, barley and rice were assessed using the same methods as for maize plants. For tea plants, we quantified the biomass of newly emerged and fully developed leaves of each plant instead of shoot biomass. We used tea geometrid larvae to assess the herbivore resistance of tea plants instead of fall armyworm larvae.

Herbivore resistance and damage assays

To measure the performance of fall armyworm caterpillars, a single starved, pre-weighed second-instar larva was individually introduced into a cylindrical mesh cage (1 cm tall and 2.4 cm in diameter). The cages were clipped onto the leaves of individual plants. The cages were moved every day to provide sufficient food for the larvae. Larval mass was determined 3 days after the start of the experiment. To quantify damage, the leaves were scanned, and the removed leaf area was determined using the software Digimizer (v.6.4.4).

To measure the performance of tea geometrid larvae on tea plants, single 3-day-old tea geometrid larvae with uniform length were selected and introduced to feed on the second fully expanded leaves. The larvae and leaves of each plant were confined with a mesh bag (10 cm long and 8 cm wide). Larval mass was determined 5 days after the start of the experiment. The leaf damage was calculated with Digimizer (v.6.4.4).

Repetition of the feedback experiment

To evaluate the robustness of feedbacks on succeeding plants, we performed a fully independent repetition of the feedback experiment. The experiment was conducted similarly to the others, with the following modifications. The natural bulk soil was collected from Posieux, Switzerland (46.7730° N, 7.1063° E)[23]. Instead of fall armyworm larvae, which were unavailable, beet armyworm larvae were used for the resistance tests. The beet armyworm larvae were confined to individual plants and left to feed freely rather than being confined to mesh cages.

Exposure frequency and feedback persistence experiment

To determine whether the HAC-triggered plant feedback effects depended on the exposure frequency, we exposed maize plants with control or HAC dispensers for 1, 2, 4 or 7 days (1.5 h per day). New B73 plants were then grown in the conditioned soils in the greenhouse and phenotyped after 25 days.

To test whether the removal time of the exposed receiver plants influences the HAC-triggered feedback effects, we removed the receiver plants 0.25 day and 1 day after control and HAC exposure. New B73 plants were then grown in the conditioned soils in the greenhouse and phenotyped after 25 days.

To explore the persistence of HAC-triggered soil feedback effects, the soils of control and HAC-exposed receiver plants were left in the greenhouse for 7, 20 and 40 days. New B73 plants were then grown in these soils in the greenhouse and phenotyped after 25 days.

Field experiments

Field trials were carried out from 2021 to 2024 in Hangzhou (eastern China; 30.2700° N, 120.1891° E), Sanya (southernmost China; 18.3117° N, 109.4498° E), Qingyang (central China; 35.3533° N, 108.0203° E) and Yazhou (southernmost China; 18.3716° N, 109.1891° E). These four locations have completely different soil types and climate environments.

Hangzhou has a subtropical monsoon climate and has alfisols. Sanya and Yazhou have a tropical marine climate and have oxisols. Qingyang has a semi-arid climate and has aridisols. The physical and biochemical properties of the soil in these locations are shown in Extended Data Fig. 5. The experiments were conducted in Hangzhou from May to October 2021, in Sanya from December 2021 to April 2022, in Qingyang from May to October 2022 and in Yazhou from December 2023 to April 2024.

B73 maize seeds were sown, and each field was divided into 10–12 blocks (each 6 m × 6 m). Each block was surrounded by a maize buffer zone of 1.5 m. At the V3 stage (third maize leaf fully open), the blocks were randomly assigned to control and HAC exposure treatments, resulting in five or six biological replicates per treatment. Control or HAC dispensers were placed beside the maize plants to ensure a consistent release of volatiles over time and sufficient exposure in an open-air environment. During exposure, each block was surrounded with a transparent plastic fence to minimize HAC cross-contamination. This set-up effectively mimicked the natural volatile emission patterns observed in the lab. A detailed image of the HAC exposure set-up in the field is provided in Fig. 3a.

After exposure for 3 days (1.5 h per day), the maize plants were removed, and new B73 maize plants were sown. During the vegetative growth period, the number of fall armyworm larvae in each block was counted every 6 to 7 days. To quantify the chlorophyll content, 10–30 plants were randomly selected in each plot. The chlorophyll content of the youngest fully opened leaf of each plant was measured using a SPAD-502 meter (Minolta Camera). Shoot dry weight and 1,000-seed weight were measured at the end of the experiments. Grain weight per ear was also assessed in the field experiment in Sanya.

The field experiment in Yazhou aimed to test for the effect of a full HIPV blend on PSFs. In this trial, sender maize plants were positioned adjacent to receiver maize plants, allowing the latter to naturally receive HIPVs emitted by the sender maize subjected to simulated herbivory. One day later, both the sender and receiver seedlings were removed. New maize plants (responders) were planted in the soils of the receiver plants. To ensure the robustness of our findings, different genetic backgrounds were intentionally employed for the sender, receiver and responder maize plants. The sender and receiver maize plants belonged to the Xianyu1938 hybrid cultivar, while the responder maize plant was the B73 inbred cultivar. The number of fall armyworms, chlorophyll content, shoot dry weight and 1,000-seed weight were determined as described above.

Soil analysis

Soil texture, pH, dissolved organic carbon, available nitrogen, potassium, phosphorous, copper, zinc, magnesium, manganese, iron, silicon, molybdenum and nickel in field soils were extracted and determined according to our previously described protocols[64].

Phytohormone analysis

The phytohormones OPDA, JA, JA–Ile, SA, IAA and ABA were extracted with ethyl acetate spiked with isotopically labelled standards (1 ng for d_6-JA, d_6-JA–Ile, d_4-SA, d_5-IAA and d_6-ABA) as described in a previous study[65]. The samples were analysed using an ultra-performance liquid chromatography (UPLC)–MS/MS method. UPLC separation was performed on an Acquity BEH C18 column (2.1 mm × 50 mm i.d., 1.7 µm particle size) at 35 °C. The UPLC and MS/MS conditions were set as described previously[66].

JA complementation experiment

To complement the *lox8* mutants with JA, JA was dissolved at a concentration of 200 mM in ethanol as stock solution. Prior to plant treatment, the JA stock solution was diluted to a concentration of 5 mM in lanolin paste. The stems of *lox8* mutants were individually treated with 20 µl of JA-containing (*lox8* + JA) or pure lanolin (*lox8* + lanolin) paste. The treatment resulted in JA levels of 0.1 µmol per plant. The purpose of this application was to induce systemic changes in the roots of the plants rather than to release JA into the air. Therefore, the concentration of JA in the lanolin paste was not intended to emit into the air but to facilitate direct contact with the plant tissues.

Microbial sterilization and complementation experiment

To explore the role of soil microbiota in the HAC-mediated feedback effects, bulk soil from the field was conditioned by HAC- and control-exposed receiver plants as described above. The conditioned soils were further divided into four sets. The first set was left untreated and used as a positive control. The second and third sets were sterilized by X-ray (50 kGy) at Shanghai Co-Elit Agricultural Sci Tech Company, China. The fourth set was used to obtain microorganism suspensions as follows. The soil (400 ml) was mixed thoroughly with 400 ml of autoclaved Milli-Q water. The mixtures were left to stand for 2 h to let large soil particles settle. The supernatants were then sieved through a 250-µm sieve followed by two 10-µm sieves, which can retain nematodes and spores of most species of arbuscular mycorrhiza while letting the suspended microorganisms pass through. One hundred millilitres of these microorganism suspensions was then used to complement the third set of soil, which was sterilized by X-ray. In total, we got six soil types: unsterilized control and HAC soils, sterilized control and HAC soils, and sterilized control and HAC soils complemented with microorganism suspensions. New B73 plants were then planted in the different soils and phenotyped as described in the feedback experiment. Analyses included plant shoot biomass and herbivore resistance.

Microbiota profiling

To profile changes in root-associated microbiota, rhizosphere soil of control and HAC-exposed maize plants was analysed for bacterial 16S rRNA and internal transcribed spacer (ITS) gene profiling via Illumina sequencing. Approximately 200 mg of rhizosphere soil was employed as input for DNA extraction with the FastDNA SPIN Kit for Soil (MP Biomedicals). The V4-V5 region of the bacterial 16S rRNA gene was amplified using the primers 515F (5′-GTGCCAGCMGCCGCGGTAA-3′) and 907R (5′-CCGTCAATTCCTTTGAGTTT-3′). The ITS region of fungi was amplified using the PCR primers ITS1F (5′-CTTGGTCATTTAGAGGAAGTAA-3′) and ITS2 (5′-GCTGCGTTCTTCATCGATGC-3′). PCR conditions were as follows: 98 °C for 1 min; 30 cycles at 98 °C (10 s), 50 °C (30 s) and 72 °C (30 s); and 72 °C for 5 min. PCR products were validated for correct size and absence of contamination via gel electrophoresis, followed by gel purification with the E.Z.N.A. Gel Extraction Kit (Omega) and DNA quantification. The indexed paired-end libraries were generated using the NEBNext Ultr II DNA Library Prep Kit for Illumina (New England Biolabs) following the manufacturer's recommendations, and index codes were added. The library quality was assessed on the Qubit@ 2.0 Fluorometer (Thermo Fisher Scientific) and sequenced on an Illumina HiSeq PE250 sequencing platform (Illumina) by Novogene (Novogene).

The 16S rRNA and ITS gene sequences were processed with Easy-Amplicon v.1.12 (ref. 67), which includes QIIME2 v.2020.11 (ref. 68), VSEARCH v.2.20.0 (ref. 69) and USEARCH v.11.0.667 (ref. 70). The quality of the paired-end Illumina reads was checked using FastQC v.0.11.5. VSEARCH and USEARCH were used to conduct subsequent quality control. First, paired-end reads were merged, and the sequencing name was relabelled with the sample name (fastq_mergepairs). After the primers and barcodes were removed (fastx_strip), the low-quality reads for which the error rates were higher than 1% and the redundant reads were removed using the commands fastq_filter and fastx_uniques. Unique reads with 100% similarity to the representative 16S/ITS sequences were clustered into OTUs using unoise3. By aligning OTUs to the RDP database[71], we filtered the sequences from the chimera (uchime_ref, fastx_getseqs) and the host (sintax_cutoff). Mitochondrial and chloroplast reads were removed from the bacterial datasets. Finally, the OTU table was created (otutab; id, 0.97). The taxonomic annotation was performed using USEARCH on the basis of the RDP database (sintax_cutoff,

0.6). Subsequent diversity analyses were carried out using EasyAmplicon and QIIME2. Bray–Curtis diversity measures were visualized using PCoA plots. Differences in beta diversity were assessed using a pairwise Adonis test and permutational ANOVA (999 permutations). Analysis of the differential OTU abundance and taxa was performed using Wilcoxon rank-sum tests based on OTUs with median relative abundance from each soil >0.1%, and the corresponding *P* values were corrected for multiple tests using the FDR set at 0.05 (Supplementary Data 1).

To construct co-occurrence networks, the relative abundance of the 300 most abundant bacterial genera and all the fungal genera in the control and HAC soil were used to calculate Spearman correlations. Only the edges with Spearman correlations higher than 0.8 and adjusted *P* values lower than 0.05 were retained. Gephi v.0.9.2 was used to visualize the network[72].

Isolation and complementation of root-derived bacteria

To obtain HAC-responsive bacteria in a bacterial strain collection, we vortexed the rhizosphere soils of control and HAC-exposed plants in phosphate-buffered saline buffer (E607016, Sangon Biotech) for 5 min. The homogenates were allowed to settle for 15 min, and the supernatants were filtered using filter paper and serially diluted. The resulting supernatants were plated and cultivated on 9-cm Petri dishes in tryptic soy agar (Solarbio), 1:10 (v/v) tryptic soy agar, Reasoner's 2A agar (Solarbio), Luria–Bertani (Solarbio) and 1:10 (v/v) Luria–Bertani agar. The cultivated colonies were purified by three consecutive platings on the respective solidified media for 3 days at 28 °C. The purified bacterial colonies were further validated by Sanger sequencing with both 27F (5′-'GAGTTTGATCATGGCTCAG-3′) and 1492R (5′-GGTTACCTTGTTACGACTT-3′) primers. In this way, we obtained a total of 102 bacterial strains. Bacteria that shared >98% 16S rRNA gene similarity with OTUs that were overrepresented in the rhizosphere of HAC-treated plants were chosen for inoculation experiments. In total, we selected 18 HAC rhizosphere-enriched bacteria for the inoculation experiments (Supplementary Data 2).

To test whether the selected bacteria promote the growth and resistance of maize plants, individual strains were cultivated and added to the maize rhizosphere. Briefly, bacteria were cultured for 2 days in their respective liquid medium with a shaker (180 rpm, 28 °C) and harvested by centrifugation (5,000 *g*, 10 min). The centrifugated bacteria were washed three times in buffer solution (10 mM $MgSO_4$) and then suspended to 1×10^7 cfu ml^{-1}. Five millilitres of each bacteria suspension was drenched into the soil around pre-germinated B73 seeds. The buffer solution was used as a control. The shoot biomass, herbivore resistance and leaf damage area of maize plants were quantified 25 days after planting.

To determine whether soil bacteria can restore the feedbacks triggered by HAC exposure, we selected four bacteria strains (*Bacillus pacificus* strain2, *Priestia aryabhattai*, *Priestia koreensis* and *Rossellomorea marisflavi*) to complement the control soil. The procedures of bacterial preparation and inoculation were the same as described above. Control and HAC soils inoculated with buffer solution (10 mM $MgSO_4$) were used as positive controls. Twenty-five days after planting, shoot biomass, herbivore resistance and leaf damage area of the succeeding maize plants were evaluated.

Transcriptome profiling of succeeding maize plants

To explore the signalling components that translated changes in soil bacteria into PSFs, the roots of succeeding maize growing in control and HAC soil were individually harvested for RNA-seq analysis. Total RNA was extracted with an RNAprep Pure Plant Kit (TIANGEN). The indexed paired-end RNA-seq libraries were constructed according to the manufacturer's protocol using the Illumina NEBNext Ultr RNA Library Prep Kit (Illumina). RNA sequencing using an Illumina NovaSeq-PE150 Platform (Illumina) was completed by Novogene (Novogene). After low-quality read removal, the remaining reads were aligned to the maize B73 reference genome (RefGen_v5) sequence assembly with HISAT2 (ref. 73). The read count numbers of fragments per kilobases per million reads were converted using Stringtie v.2.1.0 software[74]. The differential expression analysis between the plants in control and HAC soil was performed was performed using DESeq2 (ref. 75). The resulting *P* values were adjusted using the Benjamini and Hochberg approach for controlling the FDR[76]. Genes with $|\log_2(\text{fold change})| \geq 1.0$ and FDR-corrected $P \leq 0.05$ were considered differentially expressed genes.

Gene expression analysis

Total RNA of maize leaves was isolated from ground leaves using the RNAprep Pure Plant Kit (TIANGEN). Three hundred nanograms of each total RNA sample was reverse transcribed with the PrimerScript RT Master Mix (Takara). The QRT (quantitative real-time)-PCR assay was performed on the LightCycler 96 Instrument (Roche) using the SYBR Green I Master (Roche Diagnostics). The actin gene Zm*Actin* was used as an internal standard to normalize cDNA concentrations. Relative gene expression levels were calculated using a $2^{-\Delta\Delta Ct}$ method. The primers used for QRT-PCR of all tested genes are listed in Supplementary Table 1.

Isolation and characterization of Zm*CRK25*

The full-length cDNA of Zm*CRK25* was amplified by PCR. The primers CRK-F (5′-ATGCAGCTGCCATTGCCATC-3′) and CRK-R (5′-TCAACGAGGGTGCAACTCAGA-3′) were designed on the basis of the sequence of Zm*CRK25* (Zm00001eb291400). PCR products were then cloned into the pEASY-blunt cloning vector (TransGen) and subsequently sequenced for verification. Structural domain prediction was carried out using the SMART (Simple Modular Architecture Research Tool) web server (http://smart.embl-heidelberg.de)[77].

Subcellular localization of ZmCRK25

For subcellular localization, the open reading frame of Zm*CRK25* without the termination codon was inserted into the pH7YWG2 plasmid, generating the ZmCRK25–EYFP fusion protein. The constructed plasmid was then transformed into *A. tumefaciens* C58C1. Subsequently, it was co-infiltrated into *N. benthamiana* leaves with C58C1 containing the mCherry plasma membrane marker plasmid[78] at an optical density of 0.7:0.7. Small living segments of *N. benthamiana* leaves were examined for fluorescence 72 hours after agroinfiltration. Fluorescence signals of EYFP and mCherry were observed and documented using confocal microscopy (Leica TCS SP5).

Feedback experiment with Zm*CRK25* knockout lines

Uniform and pre-germinated Zm*CRK25* knockout seeds were individually sown in soils in which control or HAC-exposed receiver maize plants were previously grown. The plants were taken care of as described above. The shoot biomass, herbivore resistance and leaf metabolites were determined for these new maize plants as described in the previous sections.

Statistical analysis

The data were analysed using ANOVA followed by pairwise or multiple comparisons of LSMeans, which were corrected using the FDR method. Normality was verified by inspecting residuals, and homogeneity of variance was tested through Shapiro–Wilk tests. Datasets that did not fit assumptions were log-transformed to meet the requirements of equal variance and normality. PCoA of Bray–Curtis distances was used to compare the microbiota profiles of different treatments. Significant differences between treatments were determined using Monte Carlo tests with 999 permutations. The above analyses were conducted with R v.4.2.0 using the packages car, lsmeans, vegan, RVAideMemoire, sciplot, coin, phyloseq and edgeR[79–83].

Reporting summary

Further information on research design is available in the Nature Portfolio Reporting Summary linked to this article.

Data availability

The raw sequencing data on soil microbiota and maize transcriptomes are available in the Genome Sequence Archive of the National Genomics Data Center, China National Center for Bioinformation/Beijing Institute of Genomics, Chinese Academy of Sciences (CRA023167, CRA023173 and CRA023181) and are publicly accessible at https://ngdc.cncb.ac.cn/gsa. The illustrative video that describes the protocol for HAC exposure and the subsequent determination of PSF effects on succeeding plants is available via figshare at https://doi.org/10.6084/m9.figshare.28444481 (ref. 84). Source data are provided with this paper.

Code availability

The source code used for the soil microbiota analysis is available via GitHub at https://github.com/YongxinLiu/EasyAmplicon/releases/tag/v1.12.

References

1. Loreto, F. & D'Auria, S. How do plants sense volatiles sent by other plants? *Trends Plant Sci.* **27**, 29–38 (2022).
2. Wang, N.-Q., Kong, C.-H., Wang, P. & Meiners, S. J. Root exudate signals in plant–plant interactions. *Plant Cell Environ.* **44**, 1044–1058 (2021).
3. Kessler, A., Mueller, M. B., Kalske, A. & Chautá, A. Volatile-mediated plant–plant communication and higher-level ecological dynamics. *Curr. Biol.* **33**, R519–R529 (2023).
4. Guerrieri, E. & Rasmann, S. Exposing belowground plant communication. *Science* **384**, 272–273 (2024).
5. Maurya, A. K., Patel, R. C. & Frost, C. J. Acute toxicity of the plant volatile indole depends on herbivore specialization. *J. Pest Sci.* **93**, 1107–1117 (2020).
6. Veyrat, N., Robert, C. A. M., Turlings, T. C. J. & Erb, M. Herbivore intoxication as a potential primary function of an inducible volatile plant signal. *J. Ecol.* **104**, 591–600 (2016).
7. Hu, L. Integration of multiple volatile cues into plant defense responses. *N. Phytol.* **233**, 618–623 (2022).
8. Scala, A., Allmann, S., Mirabella, R., Haring, M. A. & Schuurink, R. C. Green leaf volatiles: a plant's multifunctional weapon against herbivores and pathogens. *Int. J. Mol. Sci.* **14**, 17781–17811 (2013).
9. Schuman, M. C., Allmann, S. & Baldwin, I. T. Plant defense phenotypes determine the consequences of volatile emission for individuals and neighbors. *eLife* **4**, e04490 (2015).
10. Frost, C. J. et al. Priming defense genes and metabolites in hybrid poplar by the green leaf volatile *cis*-3-hexenyl acetate. *N. Phytol.* **180**, 722–733 (2008).
11. Karban, R., Yang, L. H. & Edwards, K. F. Volatile communication between plants that affects herbivory: a meta-analysis. *Ecol. Lett.* **17**, 44–52 (2014).
12. Heil, M. & Karban, R. Explaining evolution of plant communication by airborne signals. *Trends Ecol. Evol.* **25**, 137–144 (2010).
13. Brosset, A. & Blande, J. D. Volatile-mediated plant–plant interactions: volatile organic compounds as modulators of receiver plant defence, growth, and reproduction. *J. Exp. Bot.* **73**, 511–528 (2021).
14. Pashalidou, F. G. et al. Plant volatiles induced by herbivore eggs prime defences and mediate shifts in the reproductive strategy of receiving plants. *Ecol. Lett.* **23**, 1097–1106 (2020).
15. Freundlich, G. E., Shields, M. & Frost, C. J. Dispensing a synthetic green leaf volatile to two plant species in a common garden differentially alters physiological responses and herbivory. *Agronomy* **11**, 958 (2021).
16. Maurya, A. K., Pazouki, L. & Frost, C. J. Priming seeds with indole and (*Z*)-3-hexenyl acetate enhances resistance against herbivores and stimulates growth. *J. Chem. Ecol.* **48**, 441–454 (2022).
17. Erb, M. et al. Indole is an essential herbivore-induced volatile priming signal in maize. *Nat. Commun.* **6**, 6273 (2015).
18. Hu, L., Ye, M. & Erb, M. Integration of two herbivore-induced plant volatiles results in synergistic effects on plant defence and resistance. *Plant Cell Environ.* **42**, 959–971 (2019).
19. Riedlmeier, M. et al. Monoterpenes support systemic acquired resistance within and between plants. *Plant Cell* **29**, 1440–1459 (2017).
20. Paudel Timilsena, B., Seidl-Adams, I. & Tumlinson, J. H. Herbivore-specific plant volatiles prime neighboring plants for nonspecific defense responses. *Plant Cell Environ.* **43**, 787–800 (2020).
21. Howard, M. M., Bass, E., Chautá, A., Mutyambai, D. & Kessler, A. Integrating plant-to-plant communication and rhizosphere microbial dynamics: ecological and evolutionary implications and a call for experimental rigor. *ISME J.* **16**, 5–9 (2021).
22. Hu, L. et al. Root exudate metabolites drive plant–soil feedbacks on growth and defense by shaping the rhizosphere microbiota. *Nat. Commun.* **9**, 2738 (2018).
23. Gfeller, V. et al. Plant secondary metabolite-dependent plant–soil feedbacks can improve crop yield in the field. *eLife* **12**, e84988 (2023).
24. Dudenhöffer, J.-H., Ebeling, A., Klein, A.-M. & Wagg, C. Beyond biomass: soil feedbacks are transient over plant life stages and alter fitness. *J. Ecol.* **106**, 230–241 (2018).
25. Zhou, Y. et al. Crop rotation and native microbiome inoculation restore soil capacity to suppress a root disease. *Nat. Commun.* **14**, 8126 (2023).
26. Zhang, H. et al. Cover crop rotation suppresses root-knot nematode infection by shaping soil microbiota. *N. Phytol.* **245**, 363–377 (2025).
27. Kong, H. G., Song, G. C., Sim, H. J. & Ryu, C. M. Achieving similar root microbiota composition in neighbouring plants through airborne signalling. *ISME J.* **15**, 397–408 (2021).
28. Kong, C. H. et al. Plant neighbor detection and allelochemical response are driven by root-secreted signaling chemicals. *Nat. Commun.* **9**, 3867 (2018).
29. Christensen, S. A. et al. The maize lipoxygenase, Zm*LOX10*, mediates green leaf volatile, jasmonate and herbivore-induced plant volatile production for defense against insect attack. *Plant J.* **74**, 59–73 (2013).
30. Hu, L., Zhang, K., Wu, Z., Xu, J. & Erb, M. Plant volatiles as regulators of plant defense and herbivore immunity: molecular mechanisms and unanswered questions. *Curr. Opin. Insect Sci.* **44**, 82–88 (2021).
31. Wang, G. et al. Systemic root–shoot signaling drives jasmonate-based root defense against nematodes. *Curr. Biol.* **29**, 3430–3438 (2019).
32. Lopes, L. D., Wang, P., Futrell, S. L. & Schachtman, D. P. Sugars and jasmonic acid concentration in root exudates affect maize rhizosphere bacterial communities. *Appl. Environ. Microbiol.* **88**, e0097122 (2022).
33. Xu, J. et al. Molecular dissection of rice phytohormone signaling involved in resistance to a piercing-sucking herbivore. *N. Phytol.* **230**, 1639–1652 (2021).
34. Lebeis, S. L. et al. Salicylic acid modulates colonization of the root microbiome by specific bacterial taxa. *Science* **349**, 860–864 (2015).
35. Hannula, S. E. et al. Persistence of plant-mediated microbial soil legacy effects in soil and inside roots. *Nat. Commun.* **12**, 5686 (2021).
36. Raaijmakers, J. M. & Kiers, E. T. Rewilding plant microbiomes. *Science* **378**, 599–600 (2022).
37. Sun, Y. et al. Plant receptor-like protein activation by a microbial glycoside hydrolase. *Nature* **610**, 335–342 (2022).

38. Piovesana, M. et al. A point mutation in the kinase domain of CRK10 leads to xylem vessel collapse and activation of defence responses in *Arabidopsis*. *J. Exp. Bot.* **74**, 3104–3121 (2023).
39. Yadeta, K. A. et al. A cysteine-rich protein kinase associates with a membrane immune complex and the cysteine residues are required for cell death. *Plant Physiol.* **173**, 771–787 (2017).
40. Hoseinzadeh, A. H. et al. Comparative transcriptome provides molecular insight into defense-associated mechanisms against spider mite in resistant and susceptible common bean cultivars. *PLoS ONE* **15**, e0228680 (2020).
41. Kalske, A. et al. Insect herbivory selects for volatile-mediated plant–plant communication. *Curr. Biol.* **29**, 3128–3133 (2019).
42. Karban, R. Plant communication. *Annu. Rev. Ecol. Evol. Syst.* **52**, 1–24 (2021).
43. Ameye, M. et al. Green leaf volatile production by plants: a meta-analysis. *N. Phytol.* **222**, 666–683 (2018).
44. Wang, J., Wu, D., Wang, Y. & Xie, D. Jasmonate action in plant defense against insects. *J. Exp. Bot.* **70**, 3391–3400 (2019).
45. Frost, C. J. Information potential of an ubiquitous phytochemical cue. *N. Phytol.* **238**, 1749–1751 (2023).
46. Zhou, H. et al. Efficacy of plant growth-promoting bacteria *Bacillus cereus* YN917 for biocontrol of rice blast. *Front. Microbiol.* **12**, 684888 (2021).
47. Deng, C. et al. Molecular mechanisms of plant growth promotion for methylotrophic *Bacillus aryabhattai* LAD. *Front. Microbiol.* **13**, 4291 (2022).
48. Passera, A. et al. Characterization of *Lysinibacillus fusiformis* strain S4C11: in vitro, in planta, and in silico analyses reveal a plant-beneficial microbe. *Microbiol. Res.* **244**, 126665 (2021).
49. Planchamp, C., Glauser, G. & Mauch-Mani, B. Root inoculation with *Pseudomonas putida* KT2440 induces transcriptional and metabolic changes and systemic resistance in maize plants. *Front. Plant Sci.* **5**, 719 (2015).
50. Nomura, K. et al. A bacterial virulence protein suppresses host innate immunity to cause plant disease. *Science* **313**, 220–223 (2006).
51. Abramovitch, R. B. & Martin, G. B. Strategies used by bacterial pathogens to suppress plant defenses. *Curr. Opin. Plant Biol.* **7**, 356–364 (2004).
52. Jiang, Q. et al. Two leucine-rich repeat receptor-like kinases initiate herbivory defense responses in tea plants. *Hortic. Res.* **12**, uhae281 (2025).
53. Frisvold, G. B. How low can you go? Estimating impacts of reduced pesticide use. *Pest Manage. Sci.* **75**, 1223–1233 (2019).
54. Czepak, M. P. et al. Mechanical damage in the tillering, development and productivity of wheat. *Int. J. Plant Soil Sci.* **26**, 1–7 (2019).
55. ul Hassan, M. N., Zainal, Z. & Ismail, I. Green leaf volatiles: biosynthesis, biological functions and their applications in biotechnology. *Plant Biotechnol. J.* **13**, 727–739 (2015).
56. von Merey, G. et al. Dispensing synthetic green leaf volatiles in maize fields increases the release of sesquiterpenes by the plants, but has little effect on the attraction of pest and beneficial insects. *Phytochemistry* **72**, 1838–1847 (2011).
57. Liu, H. J. et al. High-throughput CRISPR/Cas9 mutagenesis streamlines trait gene identification in maize. *Plant Cell* **32**, 1397–1413 (2020).
58. Maag, D. et al. 3-β-D-Glucopyranosyl-6-methoxy-2-benzoxazolinone (MBOA-*N*-Glc) is an insect detoxification product of maize 1,4-benzoxazin-3-ones. *Phytochemistry* **102**, 97–105 (2014).
59. Ye, M. et al. A constitutive serine protease inhibitor suppresses herbivore performance in tea (*Camellia sinensis*). *Hortic. Res.* **10**, uhad178 (2023).
60. Ye, M. et al. Indole primes defence signalling and increases herbivore resistance in tea plants. *Plant Cell Environ.* **44**, 1165–1177 (2021).
61. Ye, M., Glauser, G., Lou, Y., Erb, M. & Hu, L. Molecular dissection of early defense signaling underlying volatile-mediated defense regulation and herbivore resistance in rice. *Plant Cell* **31**, 687–698 (2019).
62. Erb, M. et al. Signal signature of aboveground-induced resistance upon belowground herbivory in maize. *Plant J.* **59**, 292–302 (2009).
63. Chuang, W. P. et al. Herbivore cues from the fall armyworm (*Spodoptera frugiperda*) larvae trigger direct defenses in maize. *Mol. Plant Microbe Interact.* **27**, 461–470 (2014).
64. Hu, L. et al. Soil chemistry determines whether defensive plant secondary metabolites promote or suppress herbivore growth. *Proc. Natl Acad. Sci. USA* **118**, e2109602118 (2021).
65. Glauser, G., Vallat, A. & Balmer, D. Hormone profiling. *Methods Mol. Biol.* **1062**, 597–608 (2014).
66. Sato, C., Seto, Y., Nabeta, K. & Matsuura, H. Kinetics of the accumulation of jasmonic acid and its derivatives in systemic leaves of tobacco (*Nicotiana tabacum* cv. Xanthi Nc) and translocation of deuterium-labeled jasmonic acid from the wounding site to the systemic site. *Biosci. Biotechnol. Biochem.* **73**, 1962–1970 (2009).
67. Liu, Y. et al. Easyamplicon: an easy-to-use, open-source, reproducible, and community-based pipeline for amplicon data analysis in microbiome research. *iMeta* **2**, e83 (2023).
68. Bolyen, E. et al. Reproducible, interactive, scalable and extensible microbiome data science using QIIME 2. *Nat. Biotechnol.* **37**, 852–857 (2019).
69. Rognes, T., Flouri, T., Nichols, B., Quince, C. & Mahe, F. VSEARCH: a versatile open source tool for metagenomics. *PeerJ* **4**, e2584 (2016).
70. Edgar, R. C. Search and clustering orders of magnitude faster than BLAST. *Bioinformatics* **26**, 2460–2461 (2010).
71. Cole, J. R. et al. Ribosomal Database Project: data and tools for high throughput rRNA analysis. *Nucleic Acids Res.* **42**, D633–D642 (2014).
72. Gephi: an open source software for exploring and manipulating networks. *Proc. Int. AAAI Conf. Web Soc. Media* **3**, 361–362 (2009).
73. Kim, D., Langmead, B. & Salzberg, S. L. HISAT: a fast spliced aligner with low memory requirements. *Nat. Methods* **12**, 357–360 (2015).
74. Pertea, M. et al. StringTie enables improved reconstruction of a transcriptome from RNA-seq reads. *Nat. Biotechnol.* **33**, 290–295 (2015).
75. Love, M. I., Huber, W. & Anders, S. Moderated estimation of fold change and dispersion for RNA-seq data with DESeq2. *Genome Biol.* **15**, 550 (2014).
76. Benjamini, Y. & Yekutieli, D. The control of the false discovery rate in multiple testing under dependency. *Ann. Stat.* **29**, 1165–1188 (2001).
77. Letunic, I., Khedkar, S. & Bork, P. SMART: recent updates, new developments and status in 2020. *Nucleic Acids Res.* **49**, D458–D460 (2021).
78. Nelson, B. K., Cai, X. & Nebenfuhr, A. A multicolored set of in vivo organelle markers for co-localization studies in *Arabidopsis* and other plants. *Plant J.* **51**, 1126–1136 (2007).
79. R Core Team. R: a language and environment for statistical computing. https://cran.r-project.org/doc/manuals/r-release/fullrefman.pdf (2025).
80. Herve, M. RVAideMemoire: testing and plotting procedures for biostatistics version 0.9-83-7. https://cran.r-project.org/web/packages/RVAideMemoire/ (2023).
81. Lenth, R. V. Least-squares means: the R package lsmeans. *J. Stat. Softw.* **69**, 1–33 (2016).

82. Robinson, M. D., McCarthy, D. J. & Smyth, G. K. edgeR: a Bioconductor package for differential expression analysis of digital gene expression data. *Bioinformatics* **26**, 39–140 (2010).
83. McMurdie, P. J. & Holmes, S. phyloseq: an R package for reproducible interactive analysis and graphics of microbiome census data. *PLoS ONE* **8**, e61217 (2013).
84. Hu, L. Video shows the protocol for HAC exposure and subsequent plant soil feedback experiments. *figshare* https://doi.org/10.6084/m9.figshare.28444481 (2025).

Acknowledgements

We thank R. Li at Zhejiang University for sharing the rice *aoc* mutant and its WT Xiushui11. This research was supported by the National Key Research and Development Project of China (grant no. 2021YFD1900200 to L.H.); the National Natural Science Foundation of China (grant nos 42377285 to L.H. and 32372775 to M.Y.); Zhejiang Provincial Natural Science Foundation of China (grant nos LR25C160002 to M.Y. and LR25D010001 to L.H.); Hainan Province Science and Technology Special Fund (grant no. ZDYF2024XDNY161 to L.H.); the Elite Youth Program of Chinese Academy of Agricultural Sciences; the 111 Project (grant no. B17039 to J.M.); the Swiss National Science Foundation (grant no. 200355 to M.E.); the Swiss State Secretariat for Education, Research, and Innovation (Project CANWAS to M.E.); and the University of Bern.

Author contributions

M.Y., J.X., M.E. and L.H. designed the study. J.X., M.E., C.A.M.R., M.Y., L.H., J.M.W. and J.M.R. devised the experimental design and supervised the project. L.H., K.Z., Y.X., X.Z., J.M.W., X.O., Z.W., J.M.R., Y.H., B.M., M.Y. and Z.S. collected and analysed the data. L.H., M.Y., M.E. and J.X. wrote the initial draft of the manuscript. All authors read and approved the final version.

Competing interests

The authors declare no competing interests.

Additional information

Extended data is available for this paper at https://doi.org/10.1038/s41477-025-01987-x.

Supplementary information The online version contains supplementary material available at https://doi.org/10.1038/s41477-025-01987-x.

Correspondence and requests for materials should be addressed to Lingfei Hu, Meng Ye, Matthias Erb or Jianming Xu.

Peer review information *Nature Plants* thanks Haiyan Chu, Jurgen Engelberth and the other, anonymous, reviewer(s) for their contribution to the peer review of this work.

Reprints and permissions information is available at www.nature.com/reprints.

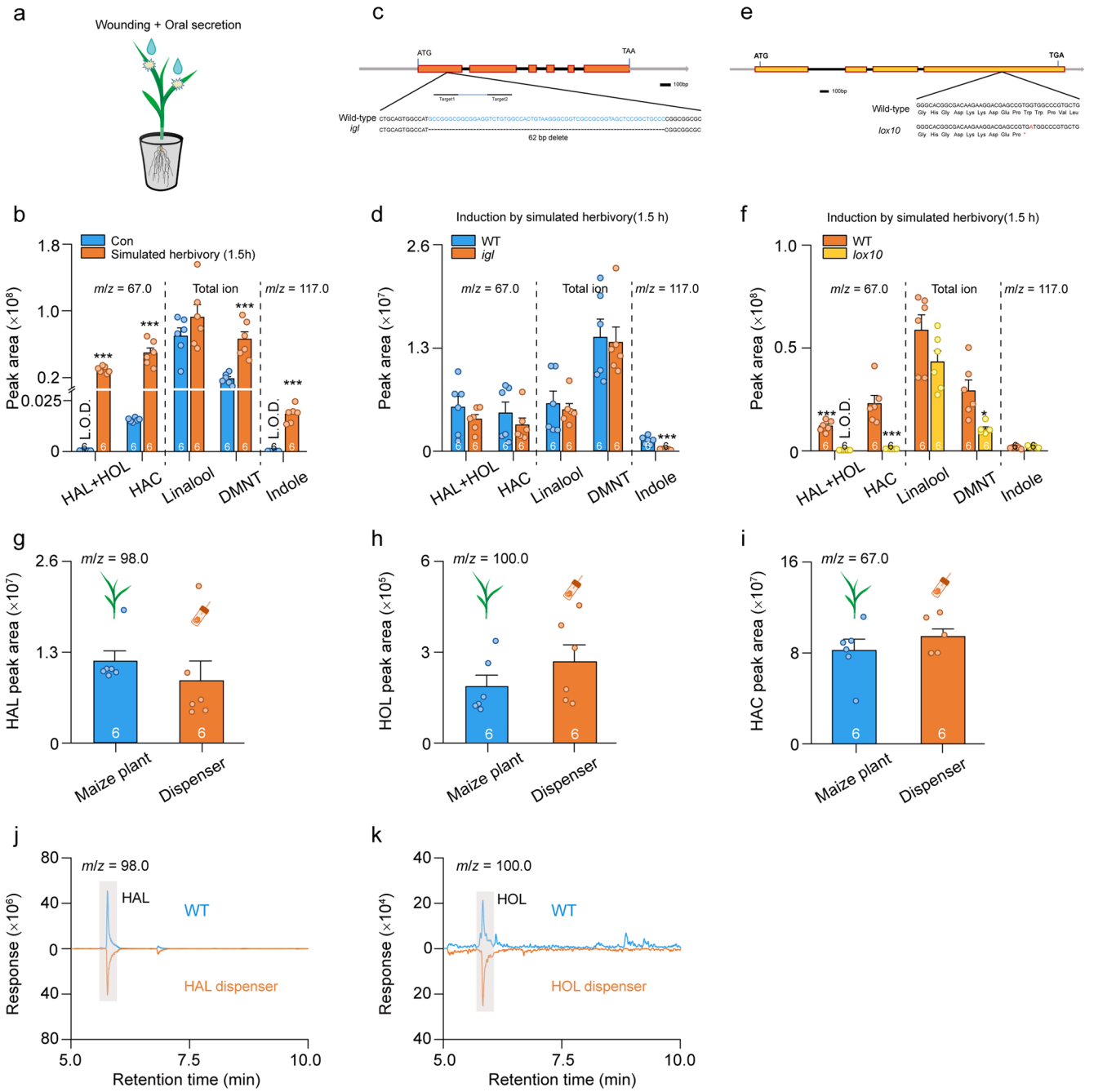
Publisher's note Springer Nature remains neutral with regard to jurisdictional claims in published maps and institutional affiliations.

Springer Nature or its licensor (e.g. a society or other partner) holds exclusive rights to this article under a publishing agreement with the author(s) or other rightsholder(s); author self-archiving of the accepted manuscript version of this article is solely governed by the terms of such publishing agreement and applicable law.

© The Author(s), under exclusive licence to Springer Nature Limited 2025

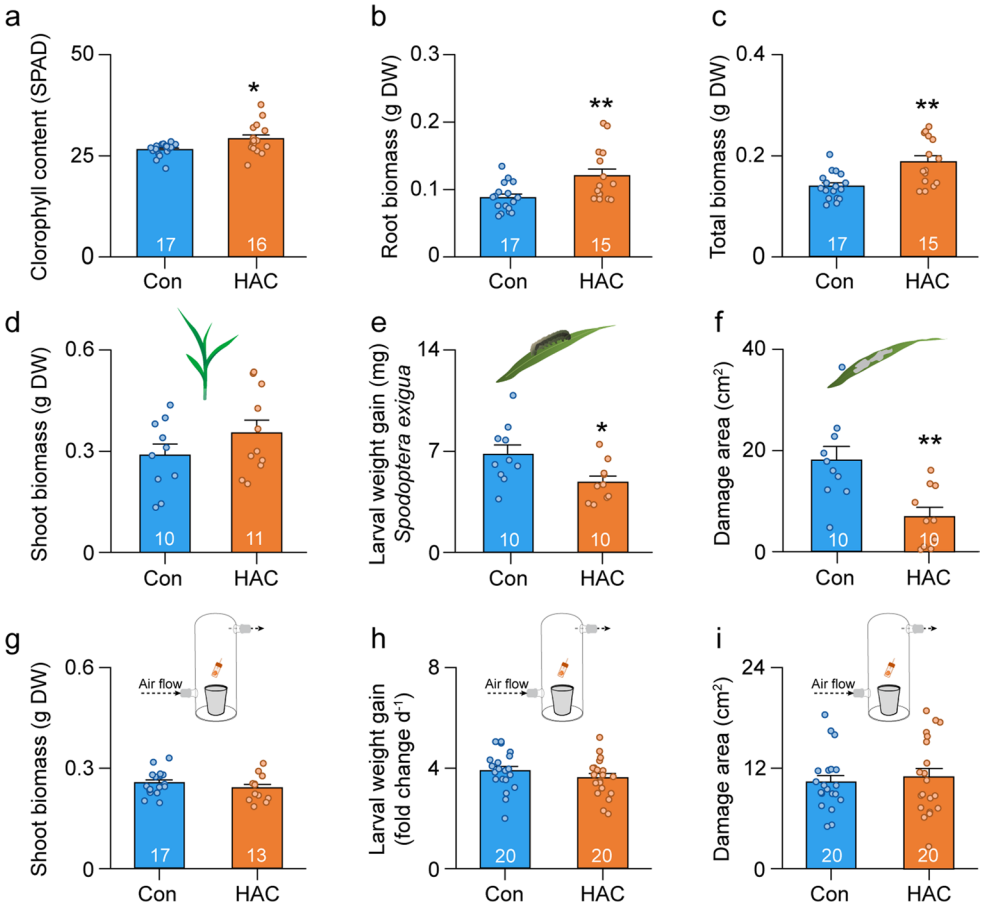
[1]State Key Laboratory of Soil Pollution Control and Safety, College of Environmental and Resource Sciences, Zhejiang Provincial Key Laboratory of Agricultural Resources and Environment, Zhejiang University, Hangzhou, China. [2]Key Laboratory of Biology, Genetics and Breeding of Special Economic Animals and Plants, Ministry of Agriculture and Rural Affairs, National Center for Tea Plant Improvement, Tea Research Institute, Chinese Academy of Agricultural Sciences, Hangzhou, China. [3]Institute of Plant Sciences, University of Bern, Bern, Switzerland. [4]Hainan Institute, Zhejiang University, Sanya, China. [5]Institute of Insect Sciences, Zhejiang University, Hangzhou, China. [6]Department of Microbial Ecology, Netherlands Institute of Ecology, Wageningen, the Netherlands. [7]Institute of Biology, Leiden University, Leiden, the Netherlands. [8]These authors contributed equally: Kaidi Zhang, Yachun Xu. ✉e-mail: lingfeihu@zju.edu.cn; yemeng@caas.cn; matthias.erb@unibe.ch; jmxu@zju.edu.cn

https://doi.org/10.1038/s41477-025-01987-x



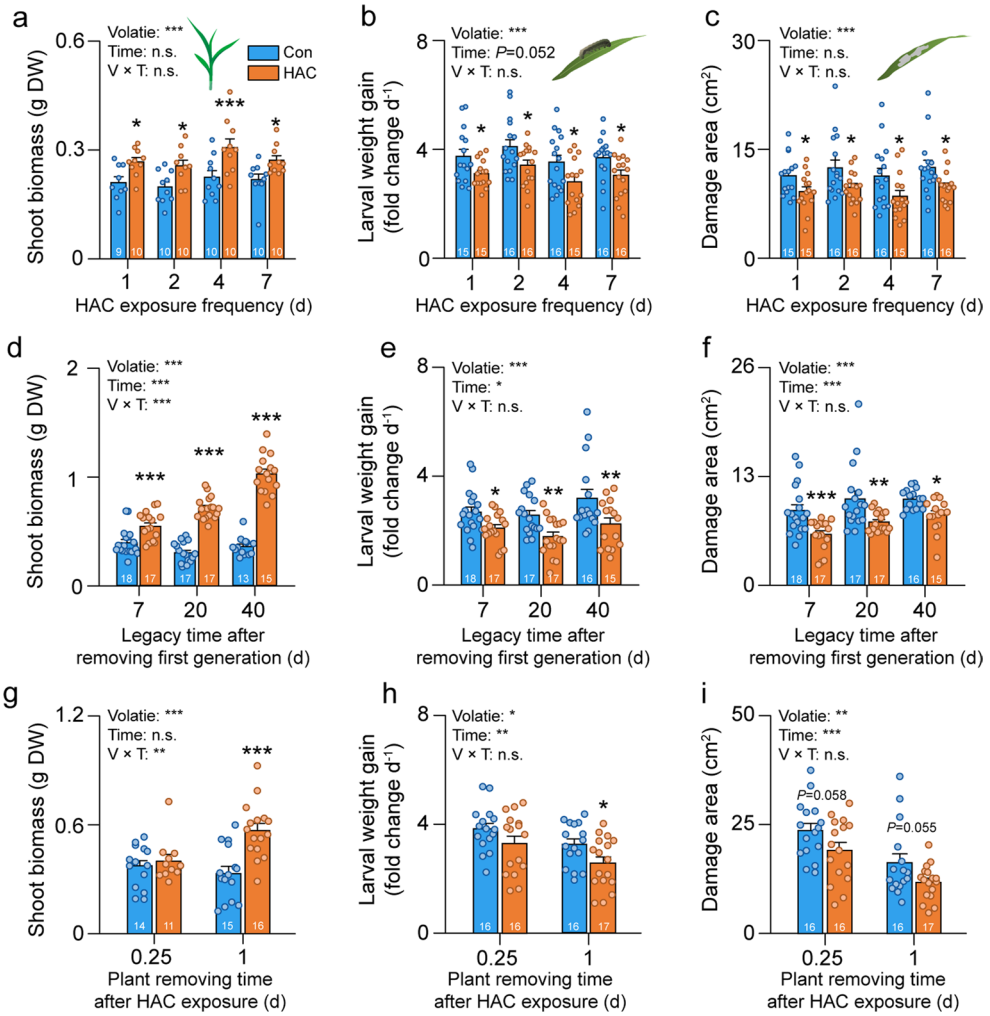
Extended Data Fig. 1 | Dispensers emit physiologically relevant levels of GLVs. a, Experimental setup of the simulated herbivory treatment. **b**, Volatile emissions from control (Con) and herbivory-induced wild-type (WT) maize plants. The herbivory-induced maize plants were treated by simulated herbivory for 1.5 h. Data are presented as mean + SEM. The exact number of biological replicates is indicated on each bar. Data points represent individual replicate samples. Asterisks denote significant differences between treatments (two-sided Student's *t* test, ***$P < 0.001$). **c**, Diagram of genomic structure of *ZmIGL* gene regions edited by CRISPR-Cas9. Bars indicate exons and lines represent introns. Scale bar represents 100 bp. **d**, Volatile emissions from WT plants and *igl* mutants that were induced by simulated herbivory for 1.5 h. Data are presented as mean + SEM. The exact number of biological replicates is indicated on each bar. Data points represent individual replicate samples. Asterisks denote significant differences between treatments (two-sided Student's *t* test, ***$P < 0.001$). **e**, Diagram of genomic structure of *ZmLOX10* gene regions with mutated position indicated. Bars indicate exons and lines represent introns. Scale bar represents 100 bp. **f**, Volatile emissions from WT plants and *lox10* mutants that were induced by simulated herbivory for 1.5 h. Data are presented as mean + SEM. The exact number of biological replicates is indicated on each bar. Data points represent individual replicate samples. Asterisks denote significant differences between treatments (two-sided Student's *t* test, *$P < 0.05$; ***$P < 0.001$). **g**–**i**, Release rate of (*Z*)-3-hexenal (HAL, **g**), (*Z*)-3-hexen-1-ol (HOL, **h**), and (*Z*)-3-hexenyl acetate (HAC, **i**) from herbivory-induced WT maize plants and capillary dispensers. Data are presented as mean + SEM. The exact number of biological replicates is indicated on each bar. Data points represent individual replicate samples. Raw data and exact *P* values for all comparisons in this figure are provided in the Source Data. **j**–**k**, GC/MS selected ion chromatograms of HAL (**j**) and HOL (**k**) emitted from herbivory-induced maize plants and capillary dispensers. DMNT, 4,8-dimethyl-1,3(*E*),7-nonatriene. L.O.D., below the limit of detection.

https://doi.org/10.1038/s41477-025-01987-x



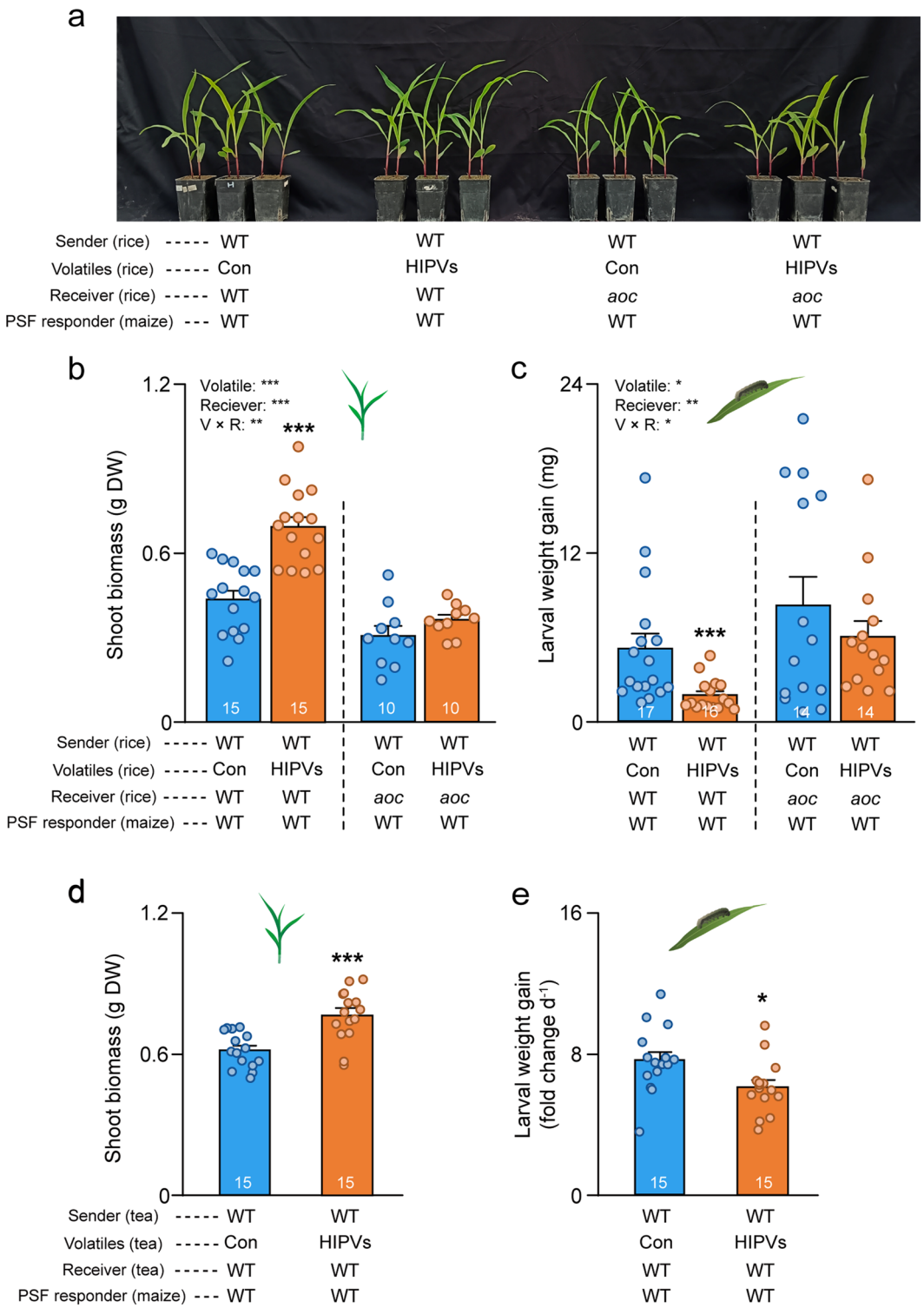
Extended Data Fig. 2 | HAC promotes maize performance via PSFs. a–**c**, Chlorophyll content (**a**), root (**b**) and total biomass (**c**) of wild-type maize plants which were growing in soils of control (Con)- or HAC-exposed receiver plants. Data are presented as mean + SEM. The exact number of biological replicates is indicated on each bar. Data points represent individual replicate samples. Asterisks denote significant differences between treatments (two-sided Student's *t* test, $^{*}P < 0.05$; $^{**}P < 0.01$). **d**–**f**, Independent repetition experiment of HAC-induced PSFs in Switzerland. Shoot biomass (**d**), larval weight gain (**e**) and leaf damage (**f**) of WT maize plants which were growing in soils of Con- or HAC-exposed receiver plants. Data are presented as mean + SEM. The exact number of biological replicates is indicated on each bar. Data points represent individual replicate samples. Asterisks denote significant differences between treatments (two-sided Student's *t* test, $^{*}P < 0.05$; $^{**}P < 0.01$). **g**–**i**, HAC triggers PSFs via a receiver plant rather than soil directly. Shoot biomass (**g**), larval weight gain (**h**) and leaf damage (**i**) of wild-type maize plants growing in soils which were directly exposed by Con or HAC volatiles. Data are presented as mean + SEM. The exact number of biological replicates is indicated on each bar. Data points represent individual replicate samples. No significant difference was observed between soil types. Raw data and exact *P* values for all comparisons in this figure are provided in the Source Data.

https://doi.org/10.1038/s41477-025-01987-x



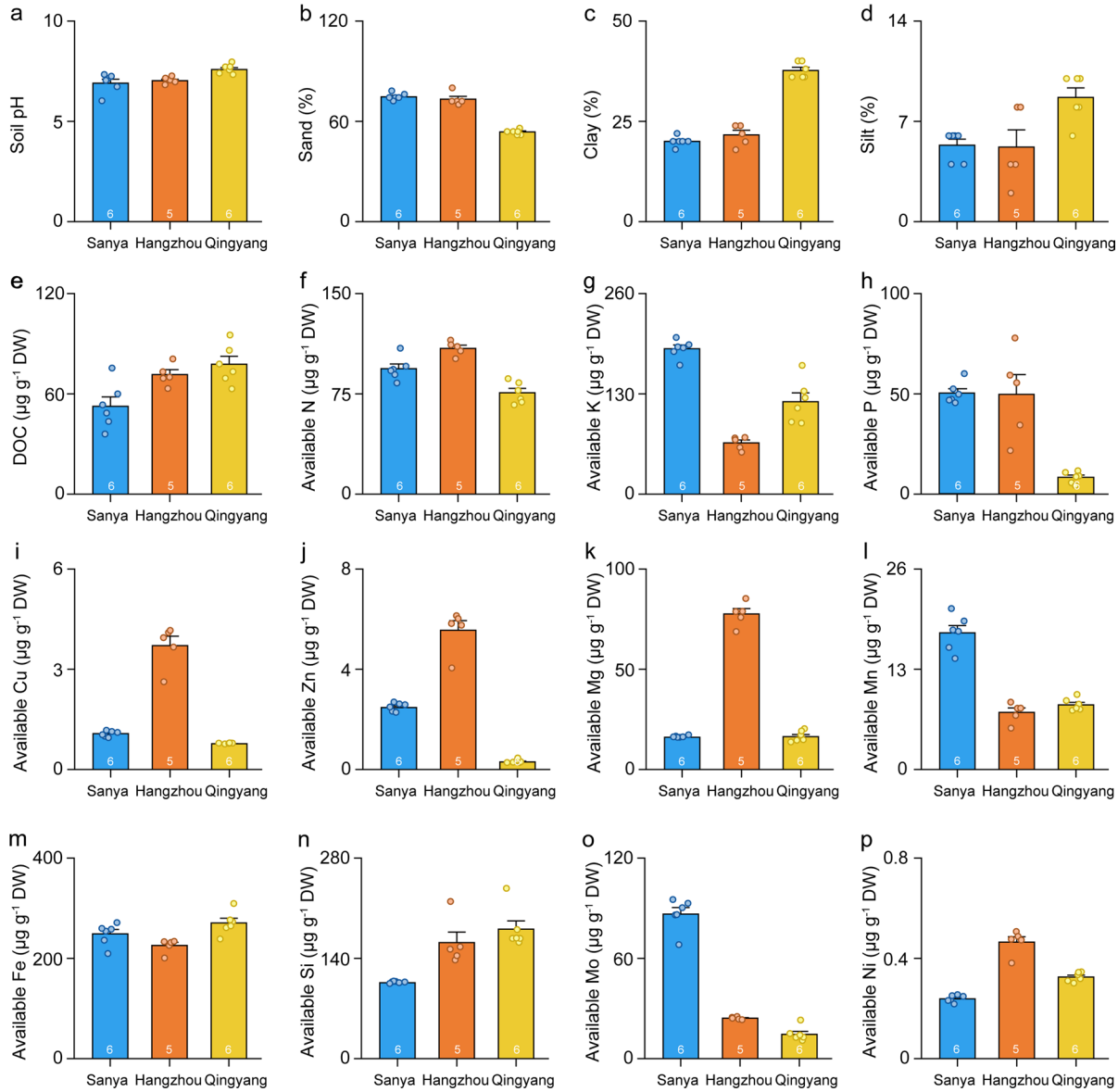
Extended Data Fig. 3 | The influences of exposure frequency, removing and legacy time on PSFs. a–**c**, Shoot biomass (**a**), larval weight gain (**b**) and leaf damage (**c**) of wild-type maize plants growing in soils of Con- or HAC-exposed receiver plants. The HAC exposure frequency over different consecutive days was indicated. Data are presented as mean + SEM. The exact number of biological replicates is indicated on each bar. Data points represent individual replicate samples. Asterisks denote significant differences between treatments (ANOVA followed by pairwise comparisons of FDR-corrected LSMeans, $^{*}P < 0.05$; $^{***}P < 0.001$). **d**–**f**, Shoot biomass (**d**), larval weight gain (**e**) and leaf damage (**f**) of wild-type maize plants growing in soils of Con- or HAC-exposed receiver plants. The soils were left in greenhouse with different days after removing the receiver plants. Data are presented as mean + SEM. The exact number of biological replicates is indicated on each bar. Data points represent individual replicate samples. Asterisks denote significant differences between treatments (ANOVA followed by pairwise comparisons of FDR-corrected LSMeans, $^{*}P < 0.05$; $^{**}P < 0.01$; $^{***}P < 0.001$). **g**–**i**, Shoot biomass (**g**), larval weight gain (**h**) and leaf damage (**i**) of wild-type maize plants growing in soils of Con- or HAC-exposed receiver plants which were removed at different times after exposure. Data are presented as mean + SEM. The exact number of biological replicates is indicated on each bar. Data points represent individual replicate samples. Asterisks denote significant differences between treatments (ANOVA followed by pairwise comparisons of FDR-corrected LSMeans, $^{*}P < 0.05$; $^{**}P < 0.01$; $^{***}P < 0.001$). Raw data and exact *P* values for all comparisons in this figure are provided in the Source Data.

https://doi.org/10.1038/s41477-025-01987-x



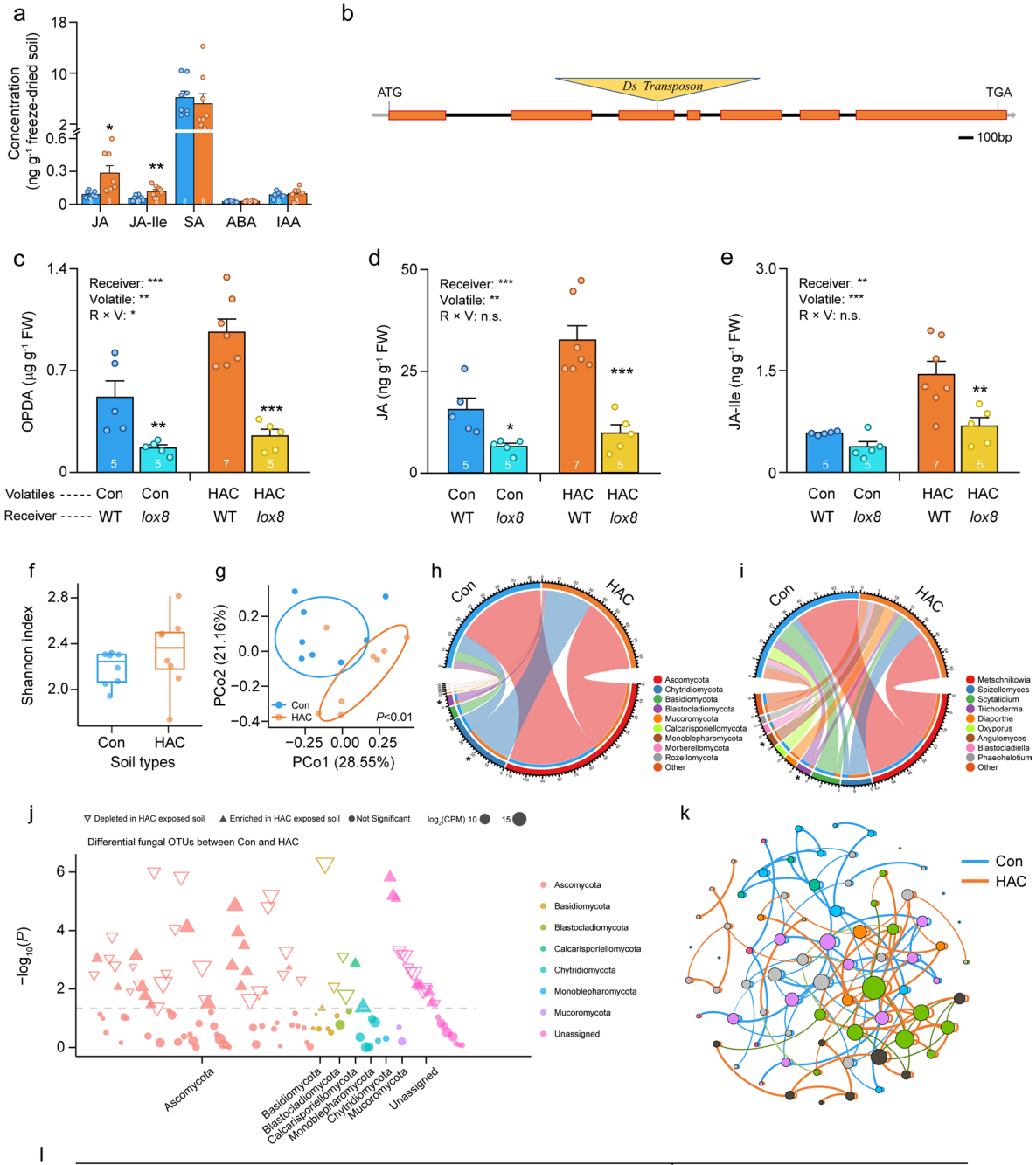
Extended Data Fig. 4 | Herbivory-induced plant volatiles (HIPVs) from rice or tea plants promote the performance and resistance of succeeding maize plants. a–**c**, Growth phenotypes (**a**), shoot biomass (**b**), caterpillar weight gain (**c**) of wild-type (WT) maize plants growing in soils of Con- or HIPV-exposed rice WT plants or *aoc* mutants. Data are presented as mean + SEM. The exact number of biological replicates is indicated on each bar. Data points represent individual replicate samples. Asterisks denote significant differences between treatments (ANOVA followed by pairwise comparisons of FDR-corrected LSMeans, $^{*}P < 0.05$; $^{**}P < 0.01$; $^{***}P < 0.001$). **d**–**e**, Shoot biomass (**d**) and caterpillar weight gain (**e**) of WT maize plants growing in soils of Con- or HIPV-exposed tea receiver plants. Data are presented as mean + SEM. The exact number of biological replicates is indicated on each bar. Data points represent individual replicate samples. Asterisks denote significant differences between treatments (two-sided Student's *t* test, $^{*}P < 0.05$; $^{***}P < 0.001$). Raw data and exact *P* values for all comparisons in this figure are provided in the Source Data.

https://doi.org/10.1038/s41477-025-01987-x



Extended Data Fig. 5 | Chemical and physical properties of field soils. The soil pH (**a**), content of sand (**b**), clay (**c**), silt (**d**), dissolved organic carbon (DOC, **e**), available nitrogen (N, **f**), potassium (K, **g**), phosphorous (P, **h**), copper (Cu, **i**), zinc (Zn, **j**), magnesium (Mg, **k**), manganese (Mn, **l**), iron (Fe, **m**), silicon (Si, **n**), molybdenum (Mo, **o**) and nickel (Ni, **p**) in field soils. Data are presented as mean + SEM. The exact number of biological replicates is indicated on each bar. Data points represent individual replicate samples. Raw data for this figure are provided in the Source Data. DW, dry weight.

https://doi.org/10.1038/s41477-025-01987-x



l

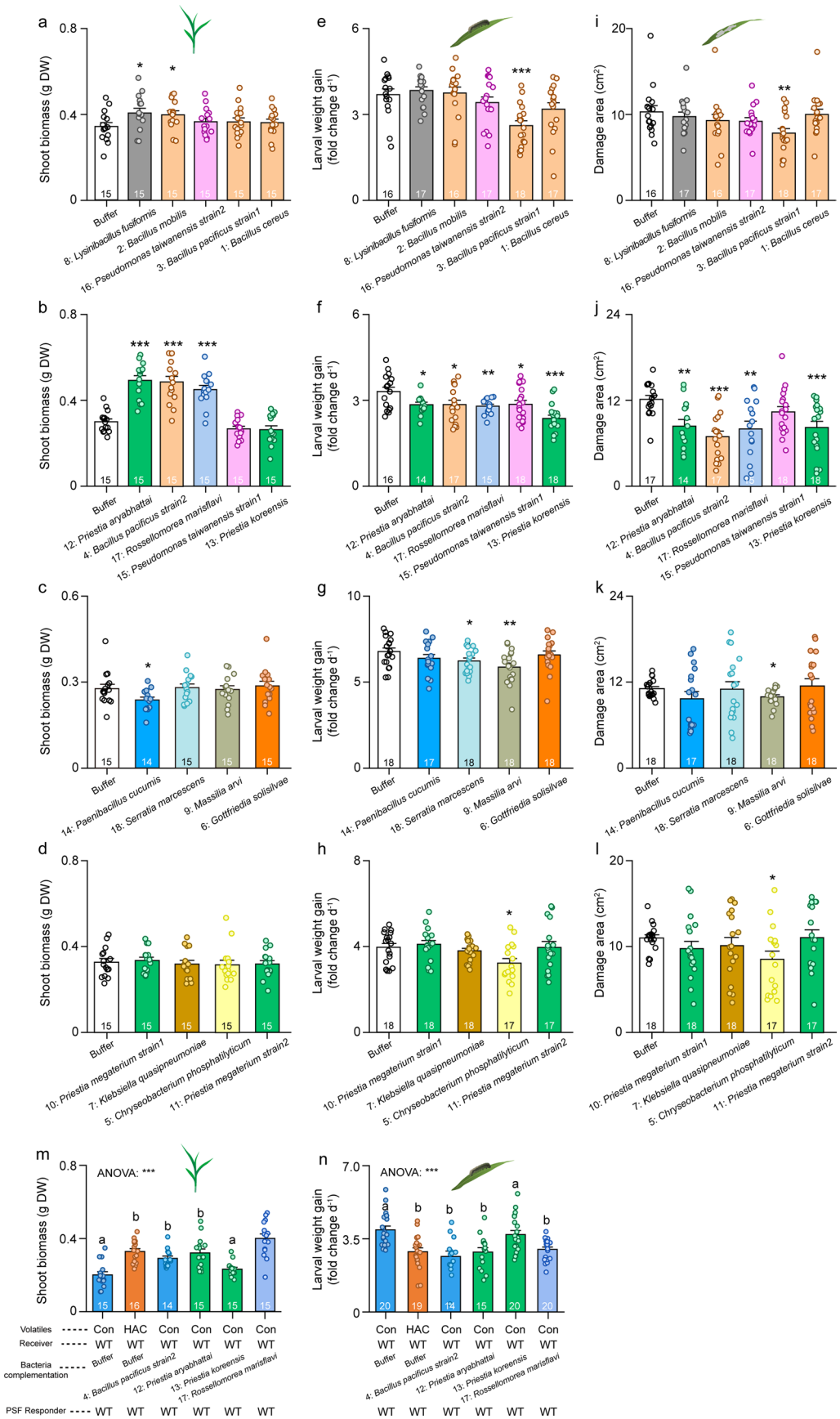
Soil type	Bacteria		Fungus	
	Con	HAC	Con	HAC
Modularity	2.993	5.269	2.588	2.363
Nodes	299	300	39	37
Number of edges	1880	1906	89	94
Average degree	12.575	12.707	4.564	5.081
Average weighted degree	3.341	2.815	2.251	2.395
Network diameter	10	9	9	9
Average path length	3.607	3.74	3.86	3.246
Graph density	0.042	0.042	0.120	0.141
Clustering coefficient	0.545	0.559	0.644	0.609
Degree centralization	0.058	0.091	0.090	0.164
Closeness centralization	NaN	0.161	NaN	NaN
Betweenness centralization	0.027	0.043	0.138	0.182

Extended Data Fig. 6 | See next page for caption.

https://doi.org/10.1038/s41477-025-01987-x

Extended Data Fig. 6 | Soil fungi in the rhizosphere of HAC-exposed maize receiver plants. a, The phytohormone concentrations in the rhizosphere soil of receiver plants after HAC exposure. Data are presented as mean + SEM. The exact number of biological replicates is indicated on each bar. Data points represent individual replicate samples. Asterisks denote significant differences between treatments (two-sided Student's *t* test, $^{*}P < 0.05$; $^{**}P < 0.01$). Raw data and exact *P* values for all comparisons in this panel are provided in the Source Data. **b**, The information of *lox8* maize mutant. Diagram of genomic structure of *ZmLOX8* gene with transposon insertion indicated. Bars indicate exons and lines represent introns. Scale bar represents 100 bp. **c**–**e**, Concentrations of 12-oxophytodienoic acid (OPDA, **c**), jasmonic acid (JA, **d**), and JA-isoleucine (JA-Ile, **e**) in wild-type (WT) and *lox8* mutant plants after HAC exposure. Data are presented as mean + SEM. The exact number of biological replicates is indicated on each bar. Data points represent individual replicate samples. Asterisks denote significant differences between treatments (ANOVA followed by pairwise comparisons of FDR-corrected LSMeans, $^{*}P < 0.05$; $^{**}P < 0.01$; $^{***}P < 0.001$). Raw data and exact *P* values for all comparisons in this panel are provided in the Source Data. FW, fresh weight. **f**, Shannon index of fungal communities in the rhizosphere of control (Con)- or HAC-exposed maize receiver plants There are eight biological replicates for each treatment. Data points represent individual replicate samples. **g**, Unconstrained PCoA with Bray-Curtis distance showing that the rhizosphere fungal communities of Con-exposed maize receiver plants separate from those of HAC-exposed receiver plants in the first axis ($P < 0.01$, permutational multivariate analysis of variance [PERMANOVA] by Adonis). There are eight biological replicates for each treatment. Data points represent individual replicate samples. **h**–**i**, Phylum- (**g**) and genus (**h**)-level distribution of fungus communities in the rhizosphere of Con- and HAC-exposed WT receiver plants. There are eight biological replicates for each treatment. **j**, Manhattan plot showing fungal OTUs enriched in the rhizosphere of Con- or HAC-exposed receiver plants. Each dot or triangle represents a single OTU. OTUs enriched in Con- or HAC-exposed soil are represented by filled or empty triangles, respectively. Differential OTU abundance was analyzed using two-sided Wilcoxon rank-sum tests, with P values corrected by the FDR method ($P < 0.05$). OTUs are arranged in taxonomic order and colored according to the phylum. CPM, counts per million. **k**, Rhizofungal co-occurrence networks of Con- and HAC-exposed receiver plants. The networks were constructed based on Spearman correlation analysis of taxonomic profiles ($P < 0.05$). The nodes in the network represent genus and links indicate potential microbial interactions. Node size is proportional to degree. **l**, Soil microbiota topological features of co-occurrence networks in the rhizosphere of Con- or HAC-exposed receiver plants. NaN, not a Number.

https://doi.org/10.1038/s41477-025-01987-x

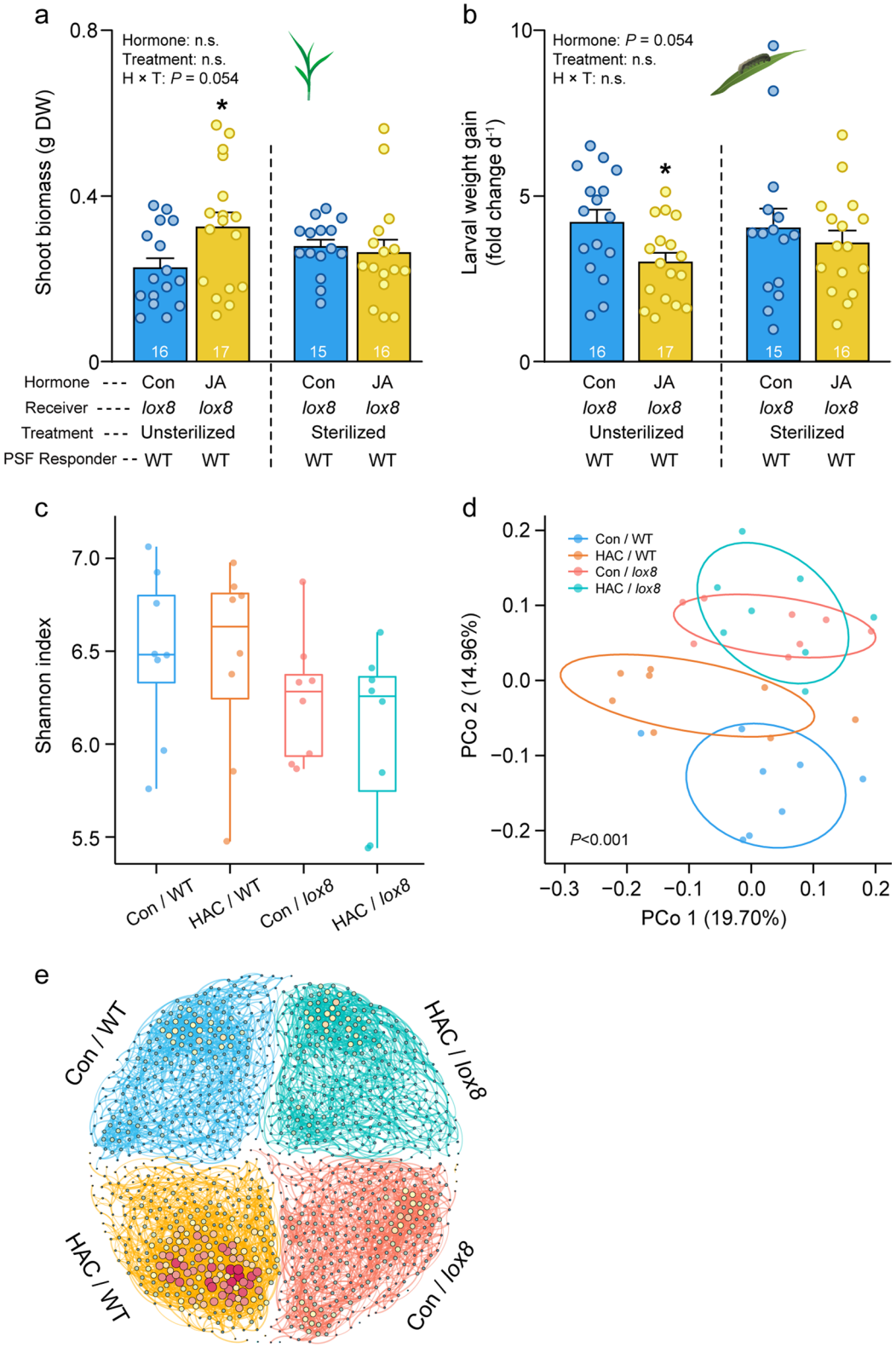


Extended Data Fig. 7 | See next page for caption.

https://doi.org/10.1038/s41477-025-01987-x

Extended Data Fig. 7 | The influence of soil bacteria on plant growth and resistance. a–**l**, Shoot biomass (**a**–**d**), larval weight gain (**e**–**h**), and leaf damage (**i**–**l**) of wild-type (WT) maize plants inoculated with 18 bacterial strains which correspond to the OTUs that are enriched in the rhizosphere of HAC-exposed plants. Data are presented as mean + SEM. The exact number of biological replicates is indicated on each bar. Data points represent individual replicate samples. Asterisks denote significant differences between bacteria inoculation and buffer treatments (two-sided Student's *t* test, $^{*}P < 0.05$; $^{**}P < 0.01$; $^{***}P < 0.001$). **m**–**n**, Bacteria complementation restores HAC-triggered PSF effects. Shoot biomass (**m**) and caterpillar weight gain (**n**) of WT maize plants growing in soils of control (Con)-exposed receiver plants. The soils were individually complemented with different bacteria strains. Data are presented as mean + SEM. The exact number of biological replicates is indicated on each bar. Data points represent individual replicate samples. Different letters denote significant differences between treatments (ANOVA followed by multiple comparisons of FDR-corrected LSMeans, $P < 0.05$). Raw data and exact *P* values for all comparisons in this figure are provided in the Source Data.

https://doi.org/10.1038/s41477-025-01987-x

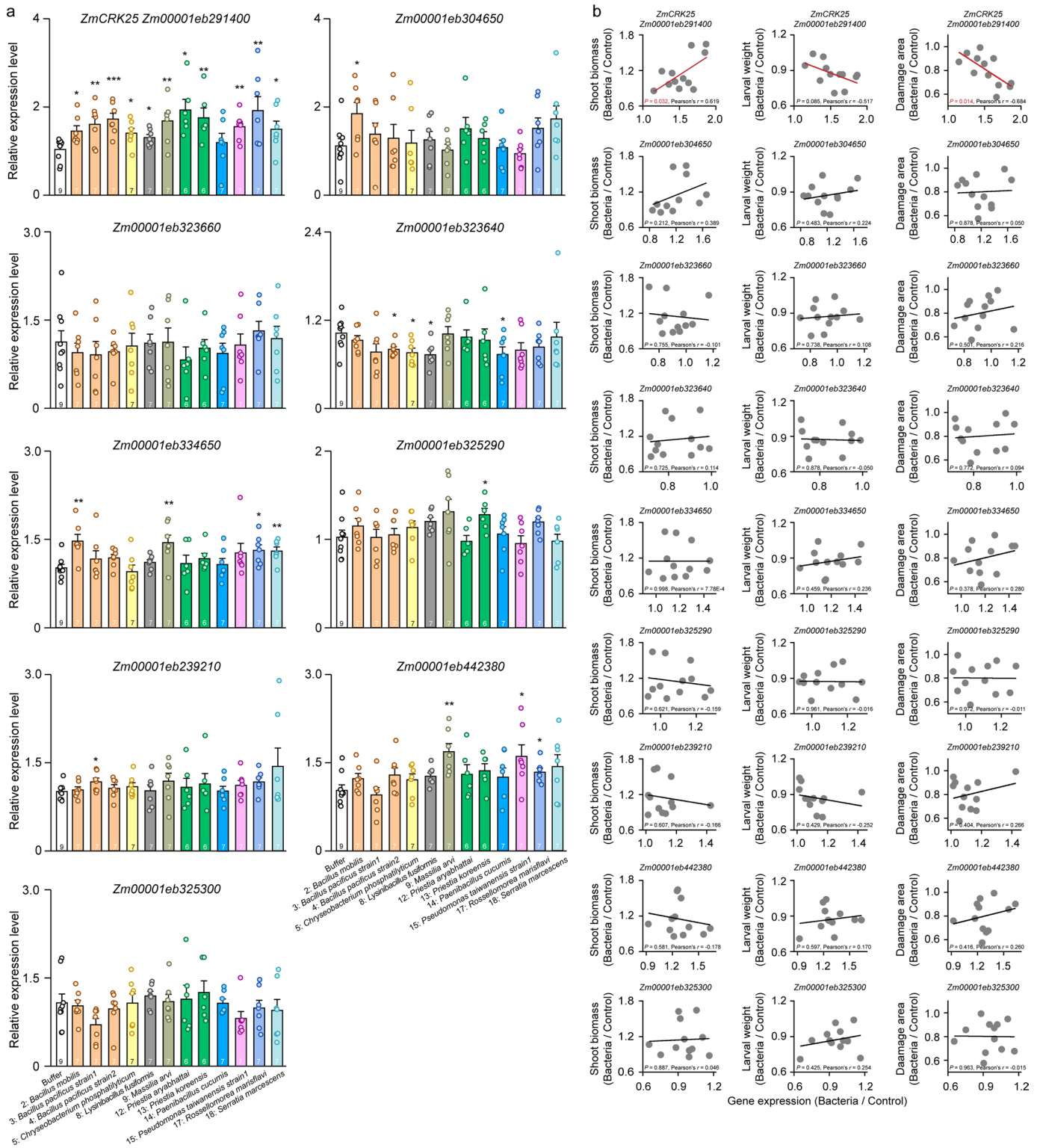


Extended Data Fig. 8 | See next page for caption.

https://doi.org/10.1038/s41477-025-01987-x

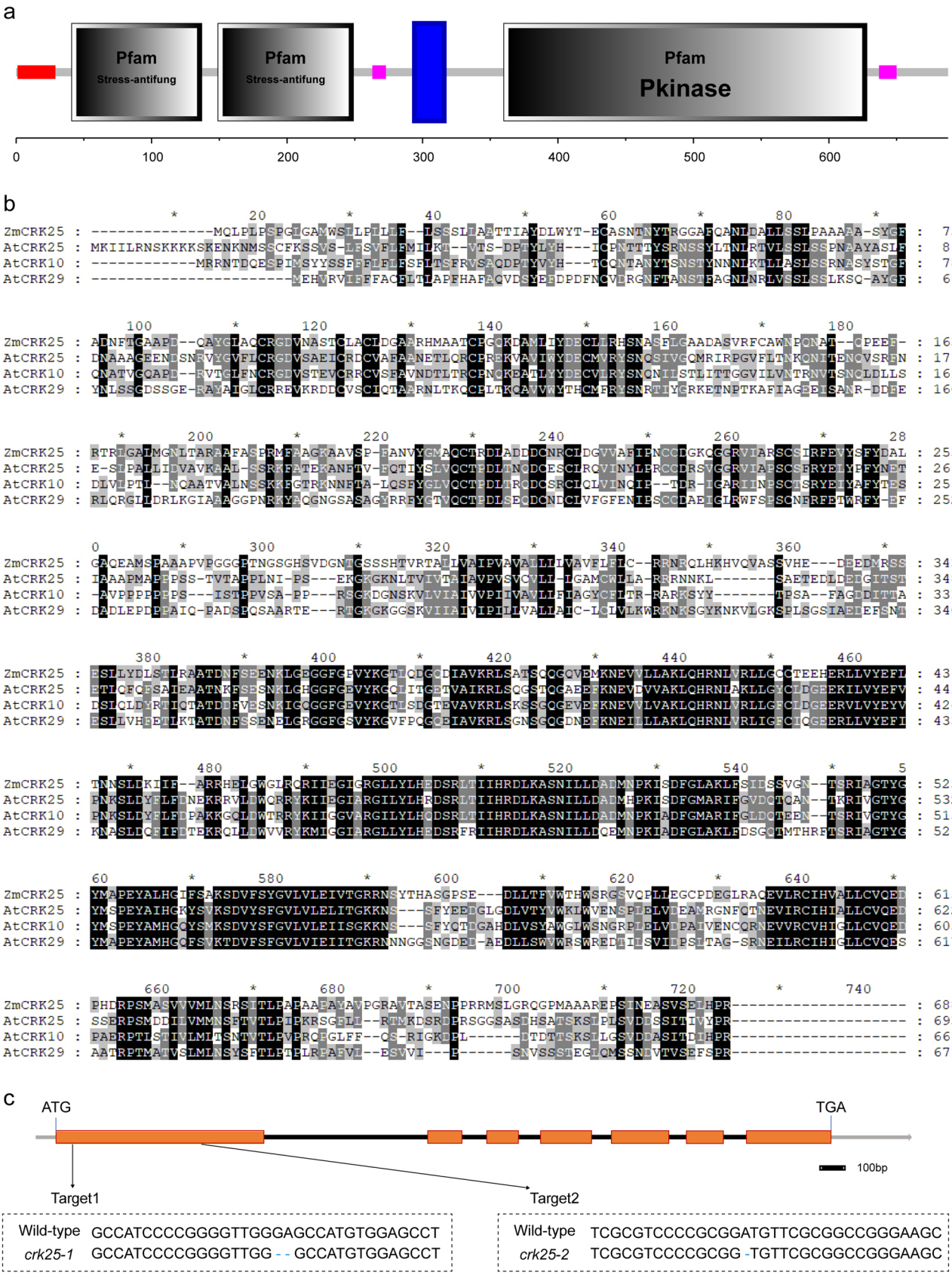
Extended Data Fig. 8 | Soil bacteria in the rhizosphere of wild-type plants and *lox8* mutants after HAC exposure. a–**b**, Shoot biomass (**a**) and caterpillar weight gain (**b**) of wild-type (WT) plants growing in soils of control (Con)- or JA-complemented *lox8* receiver plants. Data are presented as mean + SEM. The exact number of biological replicates is indicated on each bar. Data points represent individual replicate samples. Asterisks denote significant differences between treatments (ANOVA followed by pairwise comparisons of FDR-corrected LSMeans, $^{*}P < 0.05$). Raw data and exact *P* values for all comparisons in this panel are provided in the Source Data. Soils were either left untreated or X-ray sterilized. **c**, Shannon index of bacterial communities in the rhizosphere of Con- or HAC-exposed WT and *lox8* plants There are eight biological replicates for each treatment. Data points represent individual replicate samples. **d**, Unconstrained PCoA with Bray-Curtis distance of the rhizosphere bacterial communities of WT and *lox8* plants after Con or HAC exposure ($P < 0.001$, permutational multivariate analysis of variance [PERMANOVA] by Adonis). There are eight biological replicates for each treatment. Data points represent individual replicate samples. **e**, Rhizobacterial co-occurrence networks of Con- and HAC-exposed receiver plants. The networks were constructed based on Spearman correlation analysis of taxonomic profiles ($P < 0.05$). The nodes in the network represent genus and links indicate potential microbial interactions. Node size is proportional to degree.

https://doi.org/10.1038/s41477-025-01987-x



Extended Data Fig. 9 | Soil bacteria change the expression of receptor-like kinases. a, Expression levels of nine receptor-like kinase, *Zm00001eb291400*, *Zm00001eb304650*, *Zm00001eb323660*, *Zm00001eb323640*, *Zm00001eb334650*, *Zm00001eb325290*, *Zm00001eb239210*, *Zm00001eb442380* and *Zm00001eb325300*, in maize roots after inoculation with 12 bacterial strains which correspond to the OTUs that are enriched in the rhizosphere of HAC-exposed plants. Data are presented as mean + SEM. The exact number of biological replicates is indicated on each bar. Data points represent individual replicate samples. Asterisks denote significant differences between bacteria inoculation and buffer treatments (two-sided Student's *t* test, $^{*}P < 0.05$; $^{**}P < 0.01$; $^{***}P < 0.001$). Raw data and exact *P* values for all comparisons in this figure are provided in the Source Data. **b**, Correlations between bacteria-triggered plant growth, herbivore resistance and the expression of nine receptor-like kinases. Relative shoot biomass, larval weight, and damage area (bacteria/control) is correlated with relative expression levels of nine receptor-like kinase genes (bacteria/control) after inoculation with 12 bacterial strains which correspond to the OTUs that are enriched in the rhizosphere of HAC-exposed plants. Exact *P* values and Pearson's *r* of correlations are shown.

https://doi.org/10.1038/s41477-025-01987-x



Extended Data Fig. 10 | Protein alignment of ZmCRK25 with homologous proteins in Arabidopsis. a, Schematic representation of ZmCRK25 domain composition and organization based on conserved domain analysis. The numbers indicate amino acids positions of the ZmCRK25 protein domains. The positions of the signal peptide (red color), two salt stress response/antifungal domains (stress-antifung), transmembrane (blue color), protein kinase (Pkinase), and low complexity region (purple color) are shown. **b**, The amino acid sequence of ZmCRK25 was aligned by ClustalW with homologous sequences of CRKs in Arabidopsis: AtCRK25 (AT4G05200.2), AtCRK10 (AT4G23180.1), AtCRK29 (AT4G21410.3). **c**, Knockout of *ZmCRK25*. Diagram of genomic structure of *ZmCRK25* gene regions edited by CRISPR-Cas9. Bars indicate exons and lines represent introns. Scale bar represents 100 bp.

nature portfolio

Corresponding author(s): Lingfei Hu; Meng Ye; Matthias Erb; Jianming Xu

Last updated by author(s): Feb 20, 2025

Reporting Summary

Nature Portfolio wishes to improve the reproducibility of the work that we publish. This form provides structure for consistency and transparency in reporting. For further information on Nature Portfolio policies, see our Editorial Policies and the Editorial Policy Checklist.

Statistics

For all statistical analyses, confirm that the following items are present in the figure legend, table legend, main text, or Methods section.

n/a	Confirmed
☐	☒ The exact sample size (*n*) for each experimental group/condition, given as a discrete number and unit of measurement
☐	☒ A statement on whether measurements were taken from distinct samples or whether the same sample was measured repeatedly
☐	☒ The statistical test(s) used AND whether they are one- or two-sided *Only common tests should be described solely by name; describe more complex techniques in the Methods section.*
☐	☒ A description of all covariates tested
☐	☒ A description of any assumptions or corrections, such as tests of normality and adjustment for multiple comparisons
☐	☒ A full description of the statistical parameters including central tendency (e.g. means) or other basic estimates (e.g. regression coefficient) AND variation (e.g. standard deviation) or associated estimates of uncertainty (e.g. confidence intervals)
☐	☒ For null hypothesis testing, the test statistic (e.g. *F*, *t*, *r*) with confidence intervals, effect sizes, degrees of freedom and *P* value noted *Give P values as exact values whenever suitable.*
☐	☒ For Bayesian analysis, information on the choice of priors and Markov chain Monte Carlo settings
☐	☒ For hierarchical and complex designs, identification of the appropriate level for tests and full reporting of outcomes
☐	☒ Estimates of effect sizes (e.g. Cohen's *d*, Pearson's *r*), indicating how they were calculated

Our web collection on statistics for biologists contains articles on many of the points above.

Software and code

Policy information about availability of computer code

Data collection	QRT-PCR data were collected using LightCycler 96 1.1 software. For the transcriptomic data, RNA sequencing was conducted by an Illumina NovaSeq-PE150 Platform. The high-quality reads were aligned to the maize B73 reference genome sequence assembly with HISAT2. The read count numbers of fragments per kilobases per million reads were converted using Stringtie v2.1.0 software. The differential expression analysis was performed was performed using DESeq2. For the soil microbial data, microbial library was sequenced on an Illumina HiSeq PE250 sequencing platform. The 16S rRNA and ITS gene sequences were processed with EasyAmplicon v1.12, which includes QIIME2 v2020.11, VSEARCH v2.20.0, and USEARCH v11.0.667. The quality of the paired-end Illumina reads was checked by FastQC v.0.11.5. Diversity analyses were carried out using EasyAmplicon and QIIME2. The co-occurrence networks were conducted by Gephi 0.9.2.
Data analysis	The leaf damage was calculated with Digimizer (version 6.4.4). Data was analyzed by ANOVA followed by pairwise or multiple comparisons of Least Squares Means (LSMeans), which were corrected using the FDR method. Normality was verified by inspecting residuals, and homogeneity of variance was tested through Shapiro-Wilk's tests. Datasets that did not fit assumptions were log-transformed to meet the requirements of equal variance and normality. Principal coordinate analysis (PCoA) of Bray-Curtis distances were used to compare the microbiota profiles of different treatments. Significant differences between treatments were determined by Monte Carlo tests with 999 permutations. The above analyses were conducted using R 4.2.0 using the packages "car", "lsmeans", "vegan" and "RVAideMemoire", 'sciplot', 'coin', 'phyloseq' and 'edgeR'.

For manuscripts utilizing custom algorithms or software that are central to the research but not yet described in published literature, software must be made available to editors and reviewers. We strongly encourage code deposition in a community repository (e.g. GitHub). See the Nature Portfolio guidelines for submitting code & software for further information.

Data

Policy information about availability of data

All manuscripts must include a data availability statement. This statement should provide the following information, where applicable:

- Accession codes, unique identifiers, or web links for publicly available datasets
- A description of any restrictions on data availability
- For clinical datasets or third party data, please ensure that the statement adheres to our policy

The raw sequencing data of soil microbiota and maize transcriptome is available in the Genome Sequence Archive in National Genomics Data Center, China National Center for Bioinformation/Beijing Institute of Genomics, Chinese Academy of Sciences (GSA: CRA023167, CRA023173 and CRA023181) that are publicly accessible at https://ngdc.cncb.ac.cn/gsa. The illustrative videos and detailed instructions that describe the protocol for HAC exposure of maize plants and the subsequent determination of PSF effects on the succeeding plants are available from Figshare (DOI: 10.6084/m9.figshare.28444481). All data generated and/or analyzed during this study are provided in the Source Data.

Research involving human participants, their data, or biological material

Policy information about studies with human participants or human data. See also policy information about sex, gender (identity/presentation), and sexual orientation and race, ethnicity and racism.

Reporting on sex and gender	This study did not involve human participants or human data.
Reporting on race, ethnicity, or other socially relevant groupings	This study did not involve human participants or human data.
Population characteristics	This study did not involve human participants or human data.
Recruitment	This study did not involve human participants or human data.
Ethics oversight	This study did not involve human participants or human data.

Note that full information on the approval of the study protocol must also be provided in the manuscript.

Field-specific reporting

Please select the one below that is the best fit for your research. If you are not sure, read the appropriate sections before making your selection.

☐ Life sciences ☐ Behavioural & social sciences ☒ Ecological, evolutionary & environmental sciences

For a reference copy of the document with all sections, see nature.com/documents/nr-reporting-summary-flat.pdf

Life sciences study design

All studies must disclose on these points even when the disclosure is negative.

Sample size	*Describe how sample size was determined, detailing any statistical methods used to predetermine sample size OR if no sample-size calculation was performed, describe how sample sizes were chosen and provide a rationale for why these sample sizes are sufficient.*
Data exclusions	*Describe any data exclusions. If no data were excluded from the analyses, state so OR if data were excluded, describe the exclusions and the rationale behind them, indicating whether exclusion criteria were pre-established.*
Replication	*Describe the measures taken to verify the reproducibility of the experimental findings. If all attempts at replication were successful, confirm this OR if there are any findings that were not replicated or cannot be reproduced, note this and describe why.*
Randomization	*Describe how samples/organisms/participants were allocated into experimental groups. If allocation was not random, describe how covariates were controlled OR if this is not relevant to your study, explain why.*
Blinding	*Describe whether the investigators were blinded to group allocation during data collection and/or analysis. If blinding was not possible, describe why OR explain why blinding was not relevant to your study.*

Behavioural & social sciences study design

All studies must disclose on these points even when the disclosure is negative.

Study description	*Briefly describe the study type including whether data are quantitative, qualitative, or mixed-methods (e.g. qualitative cross-sectional,*

Study description	*quantitative experimental, mixed-methods case study).*
Research sample	*State the research sample (e.g. Harvard university undergraduates, villagers in rural India) and provide relevant demographic information (e.g. age, sex) and indicate whether the sample is representative. Provide a rationale for the study sample chosen. For studies involving existing datasets, please describe the dataset and source.*
Sampling strategy	*Describe the sampling procedure (e.g. random, snowball, stratified, convenience). Describe the statistical methods that were used to predetermine sample size OR if no sample-size calculation was performed, describe how sample sizes were chosen and provide a rationale for why these sample sizes are sufficient. For qualitative data, please indicate whether data saturation was considered, and what criteria were used to decide that no further sampling was needed.*
Data collection	*Provide details about the data collection procedure, including the instruments or devices used to record the data (e.g. pen and paper, computer, eye tracker, video or audio equipment) whether anyone was present besides the participant(s) and the researcher, and whether the researcher was blind to experimental condition and/or the study hypothesis during data collection.*
Timing	*Indicate the start and stop dates of data collection. If there is a gap between collection periods, state the dates for each sample cohort.*
Data exclusions	*If no data were excluded from the analyses, state so OR if data were excluded, provide the exact number of exclusions and the rationale behind them, indicating whether exclusion criteria were pre-established.*
Non-participation	*State how many participants dropped out/declined participation and the reason(s) given OR provide response rate OR state that no participants dropped out/declined participation.*
Randomization	*If participants were not allocated into experimental groups, state so OR describe how participants were allocated to groups, and if allocation was not random, describe how covariates were controlled.*

Ecological, evolutionary & environmental sciences study design

All studies must disclose on these points even when the disclosure is negative.

Study description	This study reveals that volatile-mediated plant-plant interactions trigger plant-soil feedbacks which enhance plant performance and shape agroecosystem dynamics through a set of broadly conserved mechanisms. The phenomenon expands the repertoire of biologically relevant plant-plant interactions in space and time and holds promise for the sustainable intensification of agriculture.
Research sample	Plants, soil, soil microbes and herbivores
Sampling strategy	Plant volatiles were collected with Super-Q trap. Leaf and root samples were harvested and ground in liquid nitrogen. For rhizosphere samples, soils were washed with sterile PBS, and stored at -20°C until use.
Data collection	Plant height, chlorophyll content of leaves, herbivore resistance, gene expression, phytohormones, and microbiota profiles. Data was collected by the scientists involved in this study using standard methods.
Timing and spatial scale	We exposed WT maize plants to HAC for 1.5 h. Chlorophyll content, shoot and root biomass of plants were recorded in 25 days after planting. Field trials were carried out from 2021 to 2022 in Hangzhou (eastern China; 30.2700, 120.1891) from May to October 2021, Sanya (southernmost China; 18.3117, 109.4498) from December 2021 to April 2022, Qingyang (central China; 35.3533, 108.0203) from May to October 2022, and Yazhou (southernmost China; 18.3716, 109.1891) from December 2023 to April 2024.
Data exclusions	No data was excluded.
Reproducibility	Major effects were reproduced across different experiments as positive controls and gave consistent results.
Randomization	All experiments were randomized.
Blinding	Analyses were blinded by assigning numbers instead of treatment labels to individual samples and tracing back treatment assignments after data collection.

Did the study involve field work? ☒ Yes ☐ No

Field work, collection and transport

Field conditions	Four locations of field experiments have completely different soil types and climate environments. The field in Hangzhou has a subtropical monsoon climate, and has alfisols. The field in Sanya and Yazhou has a tropical marine climate, and has oxisols. The field in Qingyang has a semi-arid climate, and has aridisols. The physical and biochemical properties of soil in three locations are shown in Extended Data Fig. 5.
Location	Field trials were carried out from 2021 to 2022 in Hangzhou (eastern China; 30.2700, 120.1891) from May to October 2021, Sanya (southernmost China; 18.3117, 109.4498) from December 2021 to April 2022, Qingyang (central China; 35.3533, 108.0203) from May to October 2022, and Yazhou (southernmost China; 18.3716, 109.1891) from December 2023 to April 2024.

Access & import/export	No permits necessary
Disturbance	The study caused no disturbances

Reporting for specific materials, systems and methods

We require information from authors about some types of materials, experimental systems and methods used in many studies. Here, indicate whether each material, system or method listed is relevant to your study. If you are not sure if a list item applies to your research, read the appropriate section before selecting a response.

Materials & experimental systems

n/a	Involved in the study
☒	☐ Antibodies
☒	☐ Eukaryotic cell lines
☒	☐ Palaeontology and archaeology
☐	☒ Animals and other organisms
☒	☐ Clinical data
☒	☐ Dual use research of concern
☐	☒ Plants

Methods

n/a	Involved in the study
☒	☐ ChIP-seq
☒	☐ Flow cytometry
☒	☐ MRI-based neuroimaging

Antibodies

Antibodies used	*Describe all antibodies used in the study; as applicable, provide supplier name, catalog number, clone name, and lot number.*
Validation	*Describe the validation of each primary antibody for the species and application, noting any validation statements on the manufacturer's website, relevant citations, antibody profiles in online databases, or data provided in the manuscript.*

Eukaryotic cell lines

Policy information about cell lines and Sex and Gender in Research

Cell line source(s)	*State the source of each cell line used and the sex of all primary cell lines and cells derived from human participants or vertebrate models.*
Authentication	*Describe the authentication procedures for each cell line used OR declare that none of the cell lines used were authenticated.*
Mycoplasma contamination	*Confirm that all cell lines tested negative for mycoplasma contamination OR describe the results of the testing for mycoplasma contamination OR declare that the cell lines were not tested for mycoplasma contamination.*
Commonly misidentified lines (See ICLAC register)	*Name any commonly misidentified cell lines used in the study and provide a rationale for their use.*

Palaeontology and Archaeology

Specimen provenance	*Provide provenance information for specimens and describe permits that were obtained for the work (including the name of the issuing authority, the date of issue, and any identifying information). Permits should encompass collection and, where applicable, export.*
Specimen deposition	*Indicate where the specimens have been deposited to permit free access by other researchers.*
Dating methods	*If new dates are provided, describe how they were obtained (e.g. collection, storage, sample pretreatment and measurement), where they were obtained (i.e. lab name), the calibration program and the protocol for quality assurance OR state that no new dates are provided.*

☐ Tick this box to confirm that the raw and calibrated dates are available in the paper or in Supplementary Information.

Ethics oversight	*Identify the organization(s) that approved or provided guidance on the study protocol, OR state that no ethical approval or guidance was required and explain why not.*

Note that full information on the approval of the study protocol must also be provided in the manuscript.

Animals and other research organisms

Policy information about studies involving animals; ARRIVE guidelines recommended for reporting animal research, and Sex and Gender in Research

Laboratory animals	Second instar Spodoptera frugiperda larva ; second instar Spodoptera exigua larva; 3-day old tea geometrid larvae
Wild animals	This study did not involve wild animals.
Reporting on sex	This study was not related to sex.
Field-collected samples	No field collected samples were used in the study.
Ethics oversight	No ethical approval was required for caterpillars of fall armyworm (Spodotera frugiperda), beet armyworm (Spodoptera exigua) and tea geometrid larvae (Ectropis oblique).

Note that full information on the approval of the study protocol must also be provided in the manuscript.

Clinical data

Policy information about clinical studies

All manuscripts should comply with the ICMJE guidelines for publication of clinical research and a completed CONSORT checklist must be included with all submissions.

Clinical trial registration	*Provide the trial registration number from ClinicalTrials.gov or an equivalent agency.*
Study protocol	*Note where the full trial protocol can be accessed OR if not available, explain why.*
Data collection	*Describe the settings and locales of data collection, noting the time periods of recruitment and data collection.*
Outcomes	*Describe how you pre-defined primary and secondary outcome measures and how you assessed these measures.*

Dual use research of concern

Policy information about dual use research of concern

Hazards

Could the accidental, deliberate or reckless misuse of agents or technologies generated in the work, or the application of information presented in the manuscript, pose a threat to:

No	Yes	
☒	☐	Public health
☒	☐	National security
☒	☐	Crops and/or livestock
☒	☐	Ecosystems
☒	☐	Any other significant area

Experiments of concern

Does the work involve any of these experiments of concern:

No	Yes	
☒	☐	Demonstrate how to render a vaccine ineffective
☒	☐	Confer resistance to therapeutically useful antibiotics or antiviral agents
☒	☐	Enhance the virulence of a pathogen or render a nonpathogen virulent
☒	☐	Increase transmissibility of a pathogen
☒	☐	Alter the host range of a pathogen
☒	☐	Enable evasion of diagnostic/detection modalities
☒	☐	Enable the weaponization of a biological agent or toxin
☒	☐	Any other potentially harmful combination of experiments and agents

Plants

Seed stocks	The lox10 mutant was obtained from the Maize EMS induced Mutant Database. The lox8 mutant was acquired from the Maize Genetics Cooperation Stock Center at University of Illinois at Urbana-Champaign. The JA-biosynthesis rice mutant aoc and its corresponding WT Xiushui11 were provided by Prof. Ran Li at Zhejiang University.
Novel plant genotypes	The knockout mutant igl and crk25 were generated according to a published protocol 55. Briefly, two 20 bp target sequences in the coding regions of ZmIGL or ZmCRK25 gene were selected, and inserted in to a pCPB-ZmUbi derived CRISPR/Cas9 binary vector. The constructed vectors were transformed into the receptor line KN5585 or B73-329 via Agrobacterium tumefaciens-mediated transformation.
Authentication	The lox10 mutant was authenticated by the Maize EMS induced Mutant Database. The lox8 mutant was was authenticated the Maize Genetics Cooperation Stock Center at University of Illinois at Urbana-Champaign. The JA-biosynthesis rice mutant aoc was authenticated by Prof. Ran Li at Zhejiang University.

ChIP-seq

Data deposition

☐ Confirm that both raw and final processed data have been deposited in a public database such as GEO.

☐ Confirm that you have deposited or provided access to graph files (e.g. BED files) for the called peaks.

Data access links *May remain private before publication.*	*For "Initial submission" or "Revised version" documents, provide reviewer access links. For your "Final submission" document, provide a link to the deposited data.*
Files in database submission	*Provide a list of all files available in the database submission.*
Genome browser session (e.g. UCSC)	*Provide a link to an anonymized genome browser session for "Initial submission" and "Revised version" documents only, to enable peer review. Write "no longer applicable" for "Final submission" documents.*

Methodology

Replicates	*Describe the experimental replicates, specifying number, type and replicate agreement.*
Sequencing depth	*Describe the sequencing depth for each experiment, providing the total number of reads, uniquely mapped reads, length of reads and whether they were paired- or single-end.*
Antibodies	*Describe the antibodies used for the ChIP-seq experiments; as applicable, provide supplier name, catalog number, clone name, and lot number.*
Peak calling parameters	*Specify the command line program and parameters used for read mapping and peak calling, including the ChIP, control and index files used.*
Data quality	*Describe the methods used to ensure data quality in full detail, including how many peaks are at FDR 5% and above 5-fold enrichment.*
Software	*Describe the software used to collect and analyze the ChIP-seq data. For custom code that has been deposited into a community repository, provide accession details.*

Flow Cytometry

Plots

Confirm that:

☐ The axis labels state the marker and fluorochrome used (e.g. CD4-FITC).

☐ The axis scales are clearly visible. Include numbers along axes only for bottom left plot of group (a 'group' is an analysis of identical markers).

☐ All plots are contour plots with outliers or pseudocolor plots.

☐ A numerical value for number of cells or percentage (with statistics) is provided.

Methodology

Sample preparation	*Describe the sample preparation, detailing the biological source of the cells and any tissue processing steps used.*
Instrument	*Identify the instrument used for data collection, specifying make and model number.*
Software	*Describe the software used to collect and analyze the flow cytometry data. For custom code that has been deposited into a community repository, provide accession details.*

Cell population abundance

Describe the abundance of the relevant cell populations within post-sort fractions, providing details on the purity of the samples and how it was determined.

Gating strategy

Describe the gating strategy used for all relevant experiments, specifying the preliminary FSC/SSC gates of the starting cell population, indicating where boundaries between "positive" and "negative" staining cell populations are defined.

☐ Tick this box to confirm that a figure exemplifying the gating strategy is provided in the Supplementary Information.

Magnetic resonance imaging

Experimental design

Design type

Indicate task or resting state; event-related or block design.

Design specifications

Specify the number of blocks, trials or experimental units per session and/or subject, and specify the length of each trial or block (if trials are blocked) and interval between trials.

Behavioral performance measures

State number and/or type of variables recorded (e.g. correct button press, response time) and what statistics were used to establish that the subjects were performing the task as expected (e.g. mean, range, and/or standard deviation across subjects).

Acquisition

Imaging type(s)

Specify: functional, structural, diffusion, perfusion.

Field strength

Specify in Tesla

Sequence & imaging parameters

Specify the pulse sequence type (gradient echo, spin echo, etc.), imaging type (EPI, spiral, etc.), field of view, matrix size, slice thickness, orientation and TE/TR/flip angle.

Area of acquisition

State whether a whole brain scan was used OR define the area of acquisition, describing how the region was determined.

Diffusion MRI ☐ Used ☐ Not used

Preprocessing

Preprocessing software

Provide detail on software version and revision number and on specific parameters (model/functions, brain extraction, segmentation, smoothing kernel size, etc.).

Normalization

If data were normalized/standardized, describe the approach(es): specify linear or non-linear and define image types used for transformation OR indicate that data were not normalized and explain rationale for lack of normalization.

Normalization template

Describe the template used for normalization/transformation, specifying subject space or group standardized space (e.g. original Talairach, MNI305, ICBM152) OR indicate that the data were not normalized.

Noise and artifact removal

Describe your procedure(s) for artifact and structured noise removal, specifying motion parameters, tissue signals and physiological signals (heart rate, respiration).

Volume censoring

Define your software and/or method and criteria for volume censoring, and state the extent of such censoring.

Statistical modeling & inference

Model type and settings

Specify type (mass univariate, multivariate, RSA, predictive, etc.) and describe essential details of the model at the first and second levels (e.g. fixed, random or mixed effects; drift or auto-correlation).

Effect(s) tested

Define precise effect in terms of the task or stimulus conditions instead of psychological concepts and indicate whether ANOVA or factorial designs were used.

Specify type of analysis: ☐ Whole brain ☐ ROI-based ☐ Both

Statistic type for inference

Specify voxel-wise or cluster-wise and report all relevant parameters for cluster-wise methods.

(See Eklund et al. 2016)

Correction

Describe the type of correction and how it is obtained for multiple comparisons (e.g. FWE, FDR, permutation or Monte Carlo).

Models & analysis

n/a	Involved in the study
☐	☐ Functional and/or effective connectivity
☐	☐ Graph analysis
☐	☐ Multivariate modeling or predictive analysis

Functional and/or effective connectivity

Report the measures of dependence used and the model details (e.g. Pearson correlation, partial correlation, mutual information).

Graph analysis

Report the dependent variable and connectivity measure, specifying weighted graph or binarized graph, subject- or group-level, and the global and/or node summaries used (e.g. clustering coefficient, efficiency, etc.).

Multivariate modeling and predictive analysis

Specify independent variables, features extraction and dimension reduction, model, training and evaluation metrics.